



The effect of the Messinian Salinity Crisis on the early diversification of the Tettigettalna cicadas

Journal:	<i>Zoologica Scripta</i>
Manuscript ID	ZSC-07-2022-0098.R1
Wiley - Manuscript type:	Original Article
Date Submitted by the Author:	06-Sep-2022
Complete List of Authors:	Costa, Gonçalo; Centre for Ecology Evolution and Environmental Changes Nunes, Vera; Centre for Ecology Evolution and Environmental Changes Marabuto, Eduardo; Centre for Ecology Evolution and Environmental Changes Mendes, Raquel; Centre for Ecology Evolution and Environmental Changes Silva, Diogo; Centre for Ecology Evolution and Environmental Changes Pons, Pere; Universitat de Girona, Departament de Ciències Ambientals Bas, Josep; Universitat de Girona, Departament de Ciències Ambientals Hertach, Thomas; Swiss Federal Institute for Forest Snow and Landscape Research WSL; Natural History Museum of Bern Paulo, Octávio; Centre for Ecology Evolution and Environmental Changes Simões, Paula; Centre for Ecology Evolution and Environmental Changes
Keywords:	Cicada, Tettigettalna, Messinian Salinity Crisis, Western Mediterranean, Phylogeny, Molecular dating
Note: The following files were submitted by the author for peer review, but cannot be converted to PDF. You must view these files (e.g. movies) online.	
SuppInfo_beast_input.xml SuppInfo_star_beast_input.xml	

SCHOLARONE™
Manuscripts

1
2
3
4
5
6
7
8
9
10
11
12
13
14
15
16
17
18
19
20
21
22
23
24
25
26
27
28
29
30
31
32
33
34
35
36
37
38
39
40
41
42
43
44
45
46
47
48
49
50
51
52
53
54
55
56
57
58
59
60**Corresponding author contact**

Name: Vera L. Nunes

Address:

Centre for Ecology, Evolution and Environmental Changes - cE3c

Faculdade de Ciências Universidade de Lisboa, 1749-016 Lisboa, Portugal

Telephone: +351 964331619

Email: vlunes@fc.ul.pt**Title**The effect of the Messinian Salinity Crisis on the early diversification of the *Tettigetta* cicadas**Full list of authors**GONÇALO J. COSTA¹, VERA L. NUNES¹, EDUARDO MARABUTO¹, RAQUEL MENDES¹, DIOGO N. SILVA¹, PERE PONS², JOSEP M. BAS², THOMAS HERTACH³, OCTÁVIO S. PAULO¹, PAULA C. SIMÕES¹**Running title**Early diversification of *Tettigetta*

COSTA et al.

Affiliations¹ Centre for Ecology, Evolution and Environmental Changes & CHANGE - Global Change and Sustainability Institute, Faculdade de Ciências, Universidade de Lisboa, Campo Grande, 1749-016 Lisboa, Portugal;² Departament de Ciències Ambientals, Universitat de Girona, Campus de Montilivi, 17003 Girona, Catalonia, Spain;³ Swiss Federal Institute for Forest, Snow and Landscape Research WSL, Zürcherstrasse 111, CH – 8903 Birmensdorf, Switzerland and Natural History Museum of Bern, Bernastrasse 15, CH – 3005 Bern, Switzerland**Corresponding author:** vlunes@fc.ul.pt

1
2
3
4 33 **Costa, G. et al (2022)** The effect of the Messinian Salinity Crisis on the early diversification of
5 34 the *Tettigettna* cicadas. *Zoologica Scripta*, 00, 000-000.
6
7

8 35
9

10 36 The current distribution patterns of many Mediterranean species are often a consequence of
11 37 large and impactful past geoclimatic events, such as the Messinian Salinity Crisis (MSC) and the
12 38 Quaternary glacial cycles. Cicadas are flying insects with poor dispersal ability, which have
13 39 experienced intense local differentiation in the Mediterranean, where the genus *Tettigettna*
14 40 has surfaced as a biogeographic model. The genus includes 10 species with species-specific
15 41 calling songs but identical morphology. All *Tettigettna* species are restricted to Southern
16 42 Iberia, with the exception of *T. estrellae* (northwest Iberia), the widespread *T. argentata*
17 43 (mainly Iberia, France and Italy) and *T. afroamissa* (Morocco). With an expanded genetic
18 44 dataset involving nuclear (*EF1α*) and mitochondrial (5' and 3' *COI* and *ATP*) loci, we
19 45 reconstructed the phylogeny of the genus and estimated divergence dates for *Tettigettna*
20 46 species under a Bayesian framework. Phylogeny with the new mitochondrial dataset was in
21 47 agreement with previous studies, whereas the nuclear *EF1α* supported *T. josei* and *T.*
22 48 *afroamissa* as monophyletic clades but lacked resolution to resolve the remaining taxa. Some
23 49 sister taxa share mitochondrial haplotypes, hinting for incomplete lineage sorting. Estimates of
24 50 divergence time settled *T. josei* as the earliest diverging lineage, likely as a pre- or early-MSC
25 51 event. As for the origin of *T. afroamissa* in Morocco, though time estimates could not entirely
26 52 rule out post-MSC dispersal, the most likely scenario points to isolation of African *Tettigettna*
27 53 after the reopening of the strait of Gibraltar. The Pleistocene glaciations that followed likely
28 54 impacted on the diversification of the remaining species of the genus in southern Iberia
29 55 refugia.
30
31
32
33
34
35
36
37
38
39
40
41
42
43
44
45
46
47
48
49
50
51
52
53
54
55
56
57
58
59
60

56

57 Per Costa et al., Centre for Ecology, Evolution and Environmental Changes (cE3c), Faculdade de
58 Ciências, Universidade de Lisboa, Campo Grande, 1749-016 Lisboa, Portugal. E-mail:
59 vl Nunes@fc.ul.pt
60

60

61

1
2
3
4 62 Keywords: Cicada, *Tettigetta*, Messinian Salinity Crisis, Western Mediterranean, phylogeny,
5 63 molecular dating.
6
7
8
9 64

11 65 1. INTRODUCTION

12
13 66
14 67 The complex historical biogeography of Western Mediterranean has been extensively studied
15 68 for many plant and animal taxa, where two major geo-climatic events have been often evoked
16 69 to explain current patterns of distribution and molecular diversity: the Pleistocene Ice Ages
17 70 (<2.6 Ma) and the Messinian Salinity Crisis (MSC) at the end of the Miocene, 5.97-5.33 Ma
18 71 (Gómez & Lunt, 2007; Hewitt, 2000, 1999; Marabuto et al., 2020; Médail & Diadema, 2009;
19 72 Schmitt, 2007, Trájer et al., 2021).

20 73 The MSC was triggered by tectonic movements that isolated the Mediterranean Sea from the
21 74 Atlantic Ocean and accompanied by climatic changes that led to several series of evaporation
22 75 cycles, progressively lowering the sea-level to its nearly complete desiccation (Krijgsman et al.,
23 76 2018, 1999; Manzi et al., 2013). Extensive land connections were formed between Europe and
24 77 North Africa during this process (see Fig. 1), functioning as land bridges for fauna and flora
25 78 exchange among the two continents (Gibert et al., 2013; Husemann et al., 2014). These
26 79 connections were suddenly interrupted when the Mediterranean basin was refilled through
27 80 the Gibraltar Strait corridor, at 5.33 Ma (Blanc, 2002). This event marked the beginning of the
28 81 Pliocene and created a sea barrier for poorly dispersive biota and triggered differentiation on
29 82 either side of the strait, contributing to the high endemism observed today in this biodiversity
30 83 hotspot (Lavergne et al., 2013; Médail & Diadema, 2009; Puissant & Sueur, 2010).

31 84 By late Pliocene, the Iberian Peninsula had already acquired its modern coastal configuration
32 85 (Elez et al., 2016; Jolivet et al., 2006), with the closest distance between Europe and Africa
33 86 found at the Gibraltar Strait (14 km, Fig. 1C). In the following period, the Pleistocene, the
34 87 Northern Hemisphere was subject to several glacial cycles which strongly affected the
35 88 distribution and survival of biota (Hewitt, 2000, 1999). The heterogeneity in topography and
36 89 habitats within the Iberian Peninsula and Maghreb enabled the survival of previously
37 90 widespread lineages into a plethora of local refugia (Tzedakis, 2009), supporting the concept of
38 91 “refugia within refugia” (Fig. 1D, Gómez & Lunt, 2007; Feliner, 2011; Martínez-Freiría et al,
39 92 2020; Miraldo et al., 2011; Petit, 2003). Nevertheless, overseas dispersal could have been
40 93 facilitated under glacial maxima by a significant drop in sea levels, which were estimated to
41
42
43
44
45
46
47
48
49
50
51
52
53
54
55
56
57
58
59
60

1
2
3
4 94 have reached over 100 m lower than today (Dumitru et al., 2021; Rohling et al., 2014). Post-
5
6 95 MSC overseas dispersal to either side of Gibraltar has been suggested for several taxa, such as
7
8 96 bellflowers (García-Aloy et al., 2017), lizards (Mendes et al., 2017), newts (Veith et al. 2004),
9
10 97 butterflies (Habel et al., 2011; Marabuto et al., 2020), beetles (Mas-Peinado et al., 2021) and
11
12 98 spittlebugs (Rodrigues et al., 2014). In some cases, however, divergence time estimates place
13
14 99 lineage split events between Europe and Africa much before the reopening of the Strait of
15
16 100 Gibraltar (see for e.g. Mendes et al., 2017; Paulo et al., 2008).

17
18 101 Cicadas (Hemiptera: Cicadidae) are a worldwide varied group of insects with over 3,000
19
20 102 species (Sanborn, 2014), characterized by low dispersal and long egg-to-adult life cycles (see
21
22 103 Table S2 in Simon et al., 2022), with 500 species belonging to the largest tribe Cicadettini
23
24 104 (Marshall et al., 2016). The Cicadettini are thought to have an Australasian origin, with two
25
26 105 smaller centers of diversity in the Mediterranean and South Africa (Marshall et al., 2016).
27
28 106 Cicadas spend multiple years underground as nymphs, contrasting with their ephemeral adult
29
30 107 winged stage above ground, generally lasting up to a few weeks in which they seek to mate
31
32 108 and lay their eggs. The male uses a unique calling mechanism to attract receptive females.
33
34 109 These calls are usually species-specific and recognized as effective for species delimitation
35
36 110 (Boulard, 2006). Although several aspects of their biology are still largely unknown, cicadas
37
38 111 make interesting models for biogeography, as exemplified by studies from New Zealand,
39
40 112 where vicariance appears to have played an important role in their diversification and
41
42 113 speciation (Arensburger et al., 2004a; Bator et al., 2021; Buckley & Simon, 2007; Marshall et
43
44 114 al., 2008).

45
46 115 In the western Mediterranean, cicadas of tribe Cicadettini have recently received some
47
48 116 attention regarding their diversity and biogeography (Hertach et al., 2015, 2016; Mendes et al.,
49
50 117 2014; Nunes et al., 2014a; Puissant & Sueur, 2010). The genus *Tettigettna* was created in
51
52 118 2010 to accommodate nine morphologically similar species of Cicadettini with distinct calling
53
54 119 songs (Puissant & Sueur, 2010), with all but one restricted to the Iberian Peninsula (see Fig.
55
56 120 1E). The only species extending its range beyond the Pyrenees is *T. argentata*, reaching
57
58 121 southern France, Italy, western Slovenia and southern Switzerland (Gogala & Gogala, 1999;
59
60 122 Hertach & Nagel, 2013; Puissant & Sueur, 2010). The biogeographic setting of the genus
123
124 123 changed with the recent discovery of *T. afroamissa*, a new species found in northern Morocco
125
126 124 and the first *Tettigettna* to be reported out of Europe (Costa et al., 2017). Ecologically and
127
128 125 morphologically analogous to the widespread *T. argentata*, this new species is allopatric to all
129
130 126 other *Tettigettna*, has a distinctive calling song and is genetically well differentiated (Costa et

1
2
3
4 127 al., 2017). The discovery of this species led to an important question: How and when did *T.*
5 128 *afroamissa* get into North Africa?
6
7 129 Sequence data available thus far to infer the phylogeny of *Tettigettalna spp.* is based on a
8 130 single mitochondrial gene, the cytochrome c oxidase I (Costa et al., 2017; Nunes et al., 2014a).
9 131 Both *Tettigettalna josei* and *T. afroamissa* stand out as the earliest diverging species of the
10 132 genus, but single-gene analysis proved as insufficient to resolve which *Tettigettalna* species
11 133 diverged in the first place (Costa et al., 2017). Mitochondrial genes evolve faster than nuclear
12 134 ones and often tell a biased story based on a maternally inheritance only (Ballard & Whitlock,
13 135 2004; Rubinoff & Holland, 2005; Shaw, 2002). Therefore, we use an extended dataset in this
14 136 study, with mitochondrial and nuclear gene coverage, and add molecular age dating
15 137 calibration to unfold the evolutionary history of early *Tettigettalna* diversification and find the
16 138 best explanation for current distribution of *T. afroamissa* in North Africa.
17
18 139 Three biogeographical scenarios can be hypothesized: The first is an overseas dispersal in
19 140 either direction, resulting in the splitting of the European and Moroccan lineages before the
20 141 onset of the MSC at 5.9 Ma. The second scenario, that of vicariance, postulates that a large
21 142 population existed across the land connection during the MSC, which was divided with the
22 143 opening of the Gibraltar Strait at the end of the MSC (5.33 Ma). The third scenario places
23 144 overseas dispersal of *Tettigettalna* from Europe to Africa as a post-MSC event, after 5.3 Ma,
24 145 which should have happened most likely during the Pleistocene glacial maxima, when sea level
25 146 was remarkably lower. To determine which of these scenarios is the most likely, we
26 147 reconstructed the phylogenetic relationships of *Tettigettalna* using two methods for species-
27 148 tree reconstruction within a Bayesian framework: gene concatenation and multispecies
28 149 coalescence (Heled & Drummond, 2010; Lambert et al., 2015; Tonini et al., 2015). The results
29 150 of both methods are discussed under these biogeographical hypotheses to determine the most
30 151 parsimonious scenario explaining *Tettigettalna spp.* distribution.
31
32
33
34
35
36
37
38
39
40
41
42
43
44
45
46
47
48
49

152

153 **2. MATERIALS AND METHODS**

154

155 **2.1 Sampling, DNA extraction and sequencing**

156

60

1
2
3
4 157 Sampling from previous *Tettigettalna* phylogenies by Nunes et al. (2014a) and Costa et al.
5
6 158 (2017) was extended with the collection of 41 new specimens in the Iberian Peninsula. Cicadas
7
8 159 were collected by hand or sweeping net and assigned to species according to their male calling
9
10 160 song. GPS data was recorded at each capture site and a front leg was removed and preserved
11
12 161 in 100% ethanol for genetic analysis (Fig. 2; Table S1, Supp. Info.). Dry specimens are stored at
13
14 162 the Department of Animal Biology of the Faculty of Sciences, University of Lisbon, Portugal.
15
16 163 Legs from the four Italian specimens of *T. argentata* included in this dataset were provided by
17
18 164 Thomas Hertach from his own collection.

19 165 Genomic DNA was isolated with the DNeasy Blood & Tissue Kit (Qiagen). Four gene fragments
20
21 166 were sequenced, with a total of 2504 base pairs (Table 1): (i) COI-Lep: 5' region of the
22
23 167 cytochrome C oxidase I (COI) mitochondrial gene; (ii) COI-CTL: 3' region of the cytochrome C
24
25 168 oxidase I (COI) mitochondrial gene; (iii) ATP: mitochondrial locus comprising tRNA-Asp gene (complete
26
27 169 complete sequence), ATPase subunit 8 gene (complete coding sequence) and ATPase subunit 6
28
29 170 gene (partial sequence) and (iv) EF-1 α : nuclear locus of Elongation Factor 1 α comprising exon2
30
31 171 (partial coding sequence), intron2 (complete sequence), exon3 (complete sequence), intron3 (complete
32
33 172 complete sequence) and exon4 (partial coding sequence). Amplification of each locus by
34
35 173 polymerase chain reaction (PCR) was performed in a total volume of 20 μ l containing 1xPCR
36
37 174 buffer (Promega), 0.6 U Taq polymerase (Promega), 2.8 mM MgCl₂, 0.10 mM dNTPs and 0.4
38
39 175 μ M of each primer (see Table S2, Supp Info. for primers sequences and sources). The standard
40
41 176 cycling conditions used were 94 $^{\circ}$ C for 3 min, 35 x (30 s at 94 $^{\circ}$ C, 30 s at the specific annealing
42
43 177 temperature as in Table S2 and 30 s at 72 $^{\circ}$ C) followed by a final elongation step at 72 $^{\circ}$ C for 10
44
45 178 min. PCR products were purified with Sureclean (Bioline) following the manufacturer
46
47 179 instructions. Purified fragments were sequenced with Big Dye Terminator v.3.1 (Applied
48
49 180 Biosystems) on MacroGen or Beckman Coulter Genomics facilities.

50
51 181 Sequences were edited in Sequencher v4.0.5 (Gene Codes Co.) to correct noisy and ambiguous
52
53 182 base calling. Mitochondrial sequences were checked for stop codons in DnaSP v5.10 (Librado &
54
55 183 Rozas, 2009). Sequences of nuclear EF-1 α found to be heterozygous in length were
56
57 184 reconstructed as in Flot et al. (2006). Haplotype phase was inferred with PHASE v2.1.1
58
59 185 (Stephens et al., 2001) with default settings and ran for 1000 iterations (ambiguities were
60
186 assigned as N if phase probability was < 0.70). A total of 262 new sequences were generated
187
188 by this study and deposited in GenBank (Table S1). This dataset was combined with 107
sequences of COI-Lep from *Tettigettalna* generated by previous works (see Table S1; Costa et

1
2
3
4 189 al., 2017; Nunes et al., 2014a; Simões et al., 2014). All the 148 *Tettigettalna spp* specimens of
5
6 190 the dataset were represented by COI-Lep sequences, whilst 61 were successfully sequenced
7
8 191 for nuclear EF-1 α and 45 were sequenced for all four DNA fragments (Table S1).
9

10 192

13 193 **2.2 Phylogenetic analysis**

14
15
16 194

17
18 195 Sequence alignments were carried out with MAFFT v7.273 (Katoh & Standley, 2013). Site
19
20 196 substitution saturation was tested in DAMBE (Xia et al., 2003; Xia & Xie, 2001) for each codon
21
22 197 position at coding sequences and found to be non-significant (p-value>0.05) for all
23
24 198 mitochondrial loci. Conversion of files from FASTA to NEXUS or PHYLIP format as well as gene
25
26 199 concatenation were performed with TriFusion (available at
27 200 <https://github.com/ODiogoSilva/TriFusion>). Maximum likelihood (ML) trees were obtained by
28
29 201 assigning each separate locus dataset a GTRCAT model, 1000 replicates and a rapid bootstrap
30
31 202 analysis (-x) on RAxML-HPC v.8 (Stamatakis, 2014). For the Bayesian inference (BI), each
32
33 203 dataset was partitioned into loci subsets and coding sequences were further partitioned into
34
35 204 codon positions. These partitions were subsequently tested and assigned an evolution model
36
37 205 on PartitionFinder v2 (Lanfear et al., 2016) under the corrected Akaike information criterion
38
39 206 (AICc), with a greedy search parameter. Bayesian inference trees were generated on MrBayes
40
41 207 v3.2.6 (Ronquist et al., 2012). Each dataset was assigned with two independent runs with four
42
43 208 chains, 5x10⁷ generations with burn-in set to the initial 25% trees and the evolution models
44
45 209 previously selected with PartitionFinder2. Parameter's convergence was checked in TRACER
46
47 210 and if confluence was not attained, runs were assigned additional 5x10⁷ generations and
48
49 211 checked again for confluence. *Hilaphura varipes*, *Cicada orni* and *Cicada barbara* were chosen
50
51 212 as outgroups (Table S1). All analyses were run as implemented on the CIPRES Science Gateway
52
53 213 (Miller et al., 2010). Output trees were visualized in FigTree
54
55 214 (<http://tree.bio.ed.ac.uk/software/figtree/>) and imaged in Inkscape.

56 215

59 216 **2.3 General approach for BEAST model optimization**

60 217

1
2
3
4 218 BEAST v.1.8.4 (Drummond et al., 2012) was used to estimate divergence times as implemented
5
6 219 in the CIPRES Science Gateway. Input files for BEAST analysis were initially assembled on
7
8 220 BEAUti (a package of BEAST) and then visually inspected or adjusted manually for substitution
9
10 221 site models not implemented on BEAUti. Initial substitution site models were the same used
11
12 222 for the BI tree analysis, *i.e* selected under an AICc criterion on PartitionFinder v2. Site models
13
14 223 with low ESS values would be discarded and the next best site model, ranked under AICc,
15
16 224 would be selected. After optimization, the selected site models were: TIM1e for the COI-CTL,
17
18 225 COI-LEP and ATP unlinked partitions; HKY+G for EF-1 α exon and HKY for EF-1 α intron. Tree
19
20 226 models were linked, with a Yule process prior, for the three mitochondrial partitions and for
21
22 227 the EF-1 α partitions. Clock models were linked for the COI partitions (COI-LEP + COI-CTL).
23
24 228 Because the parameter “ucl.d.stdev” of the EF-1 α exon partition abutted 0 on preliminary runs,
25
26 229 the clock model was changed from “uncorrelated relaxed” to a “strict clock with a lognormal
27
28 230 distribution”. The remaining partitions were assigned an uncorrelated relaxed clock, with a
29
30 231 lognormal distribution with “mean in real space” checked.

31
32 232 Fossil records of Cicadidae are scarce worldwide (reviewed by Moulds, 2018) and none is
33
34 233 adequate for clock calibration for *Tettigettalna* cicadas. Clock rate estimates for COI and EF-1 α
35
36 234 follow the ones of Marshall et al. (2016) set for phylogenetic analysis of Cicadettini with a
37
38 235 relaxed clock (analysis K - subclades), in which *Tettigettalna josei* and *T. argentata* were
39
40 236 included (see Marshall et al. (2016) Table S3- COI and Table S4 - EF-1 α subclade I). The values
41
42 237 used were M=0.01172 with S=0.288 for COI partition, M=0.001965 with S=2.0 for EF-1 α exon
43
44 238 and M=0.0075 with S=2.0 for EF-1 α intron.

45
46 239 As no calibrations were available for ATP, we assigned an uniform clock prior bound between
47
48 240 1.0×10^{-4} and 100 to this gene during preliminary runs, and afterwards inferred with a
49
50 241 lognormal clock prior assigned with M=0.0149 and S=2.0. The *Tettigettalna* clade was
51
52 242 constrained to be monophyletic, regardless of the outgroup being *Cicada orni*, *Cicada barbara*
53
54 243 or *Hilaphura varipes*. The parameter “ucl.d.stdev” was set to an exponential distribution bound
55
56 244 between 0 and 3.33. MCMC chain length was set for $2,5 \times 10^8$ iterations logging every 25000th
57
58 245 iteration and ran 6-7 times to check for repeatability.

59
60 246 Tracer v1.4 was employed to assess convergence and correct mixing of all parameters by
61
62 247 visually inspecting the .log files and securing the Effective Sample Size (ESS) of each
63
64 248 informative parameter to be over 200. Logcombiner was used to combine the replicate runs
65
66 249 with a 10% burnin of each run for the log and tree files.

250

251 **2.3.1 Time estimates with concatenation model** - The gene concatenation model relies on a
252 super-matrix of multiple concatenated loci to retrieve a species-tree. One of the shortcomings
253 of this method is that mitochondrial loci generally have more variable positions which often
254 mask the phylogenetic signal provided by nuclear loci, thus losing much of its resolution,
255 especially on deeper-level phylogenies (Rubinoff & Holland, 2005).

256 To infer divergence time, we selected a subset of 38 *Tettigettalna* samples that represented all
257 relevant branches of the phylogeny: two samples per species/lineage were selected, each
258 corresponding to the most ancestral and most recently derived haplotypes. All samples in this
259 subset were sequenced for all four loci (except for *T. afroamissa*, which couldn't be
260 successfully sequenced for COI-CTL). To implement the concatenated model in BEAST, each
261 locus was defined as a separate, unlinked site model and clock models were assigned as
262 previously stated in the general approach. Tree models were linked across nuclear and
263 mitochondrial loci, on BEAUti. The input file for this analysis can be accessed in the
264 Supplementary File: `beast_input.xml`.

265

266 **2.3.2 Time estimates with multispecies coalescence model** - Multispecies coalescence models
267 are often considered as superior to concatenation by differently weight – and unlink – nuclear
268 and mitochondrial loci, thus accounting for sources of gene and species-tree mismatch, such as
269 incomplete lineage sorting (Heled et al., 2013; Lanier & Knowles, 2015; McCormack et al.,
270 2010). For time estimates with the multispecies coalescent model, *BEAST (Heled and
271 Drummond, 2010) was used instead, which is an extension package of BEAST v.1.8.4
272 (Drummond et al., 2012). *BEAST enables the user to provide information on the ploidy of the
273 locus – *i.e* differentially weighing the mutations that occur in the slower-evolving nuclear loci
274 and the faster-evolving mitochondrial loci. Preliminary runs with the full mitochondrial and
275 nuclear datasets (148 individuals) mixed poorly, and Tracer showed low convergence among
276 most parameters, resulting in very low effective sample sizes, probably due to the lack of
277 resolution of the only nuclear gene included. Since nuclear EF-1 α only resolves *T. josei* and *T.*
278 *afroamissa* as monophyletic clades, leaving the remainder of the *Tettigettalna* as a large
279 polytomy, we decided it was best to place these under a single monophyletic entity, which was
280 named “Core *Tettigettalna*” (*i.e.* *T. argentata*, *T. estrellae*, *T. mariae*, *T. aneabi*, *T. defauti*, *T.*

1
2
3
4 281 *armandi*, *T. helianthemi* and *T. boulandi*). Model optimization was rapidly obtained with this
5
6 282 reduced trait set (*T. josei*, *T. afroamissa* and Core *Tettigettalna*). The final dataset for the
7
8 283 *BEAST analysis included 5 partitions: COI-CTL, COI-LEP, ATP, EF-1 α intron and EF-1 α exon and
9
10 284 the input file can be accessed in the Supplementary File: star_beast_input.xml.

11
12 285 Densitree was used to represent the distribution and topology of the large number of
13
14 286 generated trees, and to retrieve clade support. Time to the most recent common ancestor
15
16 287 (tMRCA) boxplots were generated in R Studio.

17
18 288

21 289 **3. RESULTS**

22
23 290

26 291 **3.1 Single and concatenated gene phylogenies**

27
28 292

29
30
31 293 Phylogenetic trees constructed for each mitochondrial locus with BI and ML are broadly
32
33 294 concordant and successfully retrieve most song-delimited species (Figures S1 and S2, Supp.
34
35 295 Info.). While mitochondrial loci efficiently reconstruct more recent relationships, all fail
36
37 296 individually to reconstruct the deep nodes amongst *Tettigettalna*, having low support values,
38
39 297 particularly the ones involving *T. josei* and *T. afroamissa*. Their relationship remains unclear
40
41 298 and even conflicting in single-gene analyses.

42
43 299 When concatenating all three mitochondrial loci, most clades defined with COI-Lep in previous
44
45 300 studies were here retrieved with both BI (Fig. 3a) and ML (Fig. S3) analyses. The concatenated
46
47 301 tree provides good support for considering *T. josei* as sister to all other *Tettigettalna*, in both BI
48
49 302 (1 pp, Fig. 3a) and ML (99% BS, Fig. S3), followed by *T. afroamissa* and the remainder of the
50
51 303 *Tettigettalna* (0.98 pp; <70% BS).

52
53 304 As in Nunes et al. (2014a), an unresolved clade in the concatenated tree joins *T. argentata*, *T.*
54
55 305 *aneabi* and *T. mariae* (BI 1pp; ML 99% BS). Regarding *T. heliathemi*, the apparent polyphyly of
56
57 306 this species was confirmed in this study, where samples of subspecies *T. h. galantei* from
58
59 307 Western Sierra Nevada, defined as type II by Nunes et al. (2014a), group with *T. boulandi* (BI
60
308 1pp). The remainder of *T. h. galantei*, referred as type I by Nunes et al. (2014a), form a well-

1
2
3
4 309 supported sister clade to *T. h. helianthemi*, as it would be expected from their song differences
5
6 310 (BI 1pp, ML 99% BS).

7
8
9 311 The enlarged sampling enabled the resolution of a standing *T. defauti* and *T. armandi* polytomy
10 312 (1 pp, Fig. 3a; 92% BS, Fig. S3). The new dataset also revealed additional lineages with marked
11
12 313 geographical structure: Sierra Nevada and Ronda & Zagra populations of *T. defauti* (0.89 pp,
13
14 314 Fig. 3a; 77% BS, Fig. S3) and Jerez and Gibraltar populations of *T. armandi* (1 pp, Fig. 3a; 94%
15
16 315 BS, Fig.S3).

17
18 316 Sequence data from the nuclear gene EF-1 α has about five times fewer parsimony-informative
19
20 317 sites than mitochondrial loci (Table 1) and 39 out of 63 sequenced individuals were
21
22 318 heterozygous for indel length (length of indels varied between 1 and 4 bases). Indels were
23
24 319 coded as N for phylogenetic analyses. Their distribution among taxa was random, without
25
26 320 diagnostic value. Both BI and ML phylogenetic reconstruction with nuclear gene EF-1 α have
27
28 321 low resolution (Fig 3b and Fig. S4). This locus fully retrieved *T. afroamissa* as well as *T. josei* as
29
30 322 monophyletic taxa, whereas the remainder of the specimens form a large and weakly
31
32 323 supported polytomy. Nevertheless, it is noteworthy that among *T. helianthemi*, while
33
34 324 mitochondrial DNA clearly defines two lineages corresponding to the two acoustically defined
35
36 325 subspecies (*T. h. helianthemi* and *T. h. galantei* Type I) and a third diverging lineage of *T. h.*
37
38 326 *galantei* (Type II) clustering with specimens of *T. bouleardi* (Fig. 3a), such genetic structure is not
39
40 327 supported by EF-1 α , where *T. bouleardi* groups with some specimens of the subspecies *T. h.*
41
42 328 *helianthemi* instead (Fig. 3b). Samples Thh645 and Thh238 of *T. h. helianthemi* actually share
43
44 329 the same EF-1 α haplotype with *T. bouleardi* samples, signaling incomplete lineage sorting
45
46 330 among these parapatric species in southern Spain.

47
48
49
50
51
52
53
54
55
56
57
58
59
60

3.2 Divergence time with concatenation method

331
332
333

334 Divergence time estimates for *Tettigettalna* nodes using BEAST are summarized in Table 2 and
335 Fig. 4. The concatenated species-tree is congruent with both the BI and ML trees of
336 mitochondrial datasets, apart from the basal relationships recovered within the core
337 *Tettigettalna*. BEAST concatenated species-tree confirms *T. josei* (from southwestern Iberia) as
338 the earliest diverging taxon (node A), between 9.6 and 2.8 Ma, with a mean age estimate of

1
2
3
4 339 5.9 Ma. The divergence of Moroccan *T. afroamissa* (node B) was estimated between 7.8 and
5
6 340 2.3 Ma, with a mean age estimate of 4.8, after the reopening of the Strait of Gibraltar. The
7
8 341 remaining taxa were arranged in two main subclades (node C) with a mean age estimate of 3.4
9
10 342 Ma, during late Pliocene. One subclade comprises *T. estrellae*, *T. bouldardi*, *T. helianthemi*
11 343 *galantei* Type II, *T. defauti* and *T. armandi* (BS=1). *Tettigettalna estrellae* remains *incertae-sedis*
12 344 within this subclade. Relationships between *T. defauti* and *T. armandi*, and between *T. bouldardi*
13 345 and *T. h. galantei* Type II remain well supported (both BS=1). Estimates place divergence of *T.*
14 346 *defauti* and *T. armandi* (node F) between 2.9 and 0.8 Ma and divergence of *T. bouldardi* from *T.*
15 347 *h. galantei* Type II (node G) between 2.1 and 0.5 Ma, both during the Pleistocene.

19
20 348 The second subclade (node H, BS=0.92) comprises the *T. argentata* species complex (*T.*
21 349 *argentata*, *T. mariae*, *T. aneabi*) together with its putative sister taxon *T. helianthemi*, including
22 350 its two recognized subspecies (*T. h. helianthemi* and *T. h. galantei* Type I). Both groups within
23 351 this subclade are well resolved (BS=1), but *T. argentata*, *T. mariae* or *T. aneabi* remain
24 352 polyphyletic. Divergence time estimates within subclade H (nodes I and J) are recent, during
25 353 the Pleistocene, between 2.5 and 0.6 Ma.

30
31 354

34 355 **3.3 Divergence time with coalescent method**

35
36 356

37
38
39 357 To make a *bona fide* estimation of the chain of events of the diversification of the
40 358 *Tettigettalna*, we estimated tMRCA of the clades definable by the nuclear dataset: *T. josei*, *T.*
41 359 *afroamissa* and Core *Tettigettalna*. Age estimates are summarized in Table 3. Because we were
42 360 working with a reduced number of ingroup taxa, we could ponder all the three possible
43 361 phylogenetic relationship scenarios within the *Tettigettalna* clade (see introduction). The
44 362 probabilities of such sub-clades are presented in Table 3 and Fig. 5. Of the three likely
45 363 phylogenetic relationship scenarios (Fig. 5), the one with *T. josei* as sister to all other species in
46 364 the genus has the highest bootstrap support (81.59%, Table 3), against the remaining which
47 365 have a combined reduced probability (<20%). The mean age estimate for the divergence of *T.*
48 366 *josei* is 6.9 Ma, before the MSC, though the 95% highest probability density intervals are wide
49 367 (Table 3). The tMRCA for the *T. afroamissa* – Core *Tettigettalna* split was estimated between

1
2
3
4 368 9.5 and 2.0 Ma, with a mean age estimate of 5.3 Ma, coinciding with the reopening of the
5
6 369 Strait of Gibraltar and the end of the MSC (Fig. 6).
7

8
9 370

11 371 **4. DISCUSSION**

12
13
14 372

16 373 **4.1 Phylogeny of *Tettigettna***

17
18
19 374

21
22 375 With this study, we used an extended set of mitochondrial sequences and obtained the first
23
24 376 nuclear data to investigate the evolution of the Mediterranean genus *Tettigettna*. These
25
26 377 small-sized and colour-cryptic cicadas occur at fairly low density, being very difficult to sample
27
28 378 without the use of acoustic location. Hence, and because females are mute and seldom seen,
29
30 379 the dataset is composed of males only. The inclusion of nuclear sequences is particularly
31
32 380 relevant to corroborate patterns found with mitochondrial data and discard potential bias in
33
34 381 male dispersal. As expected, nuclear EF-1 α had much lower diversity than mitochondrial
35
36 382 genes and lacked resolution in *Tettigettna*, though without conflicting with mitochondrial
37
38 383 phylogenies.

38
39 384 Regarding the order of lineage splitting among *Tettigettna*, our study gives support to *T. josei*
40
41 385 as sister to the remaining extant members of the genus, consistent with morphological and
42
43 386 acoustic differentiation observed for this species (Mendes et al., 2014). Nonetheless, the other
44
45 387 two phylogenetic scenarios in the species coalescent tree (i.e. subclades *T. josei* – Core
46
47 388 *Tettigettna* and *T. afroamissa* – *T. josei*) have some degree of support (8 – 9 %). Species *T.*
48
49 389 *afroamissa* and *T. argentata* are amongst the most genetically distant taxa in the phylogeny,
50
51 390 even though they share a similar calling song pattern. *Tettigettna* has no parallel with any
52
53 391 other cicada genus occurring in Iberia, being the most species rich, with species defined mainly
54
55 392 by song characterization (Puissant & Sueur, 2010). Such diversity of songs within *Tettigettna*
56
57 393 has evolved without significant morphological divergence, not even at genitalia morphology,
58
59 394 often a key trait to distinguish between closely related species, as it may prevent successful
60
395 mating of heterospecific couples (Knowles et al., 2016; Langerhans et al., 2016). A few song
396 operational taxonomic units within *Tettigettna* remain polyphyletic with the new sequence

1
2
3
4 397 data as in Nunes et al. (2014a) and Costa et al. (2017), namely the widespread *T. argentata*
5
6 398 with cryptic *T. mariae* and *T. aneabi*, which present partially overlapping distribution ranges
7
8 399 (Nunes et. al, 2014b). Insect songs are genetically inherited but the genes ruling them remain
9
10 400 poorly known, in particular for cicadas (Fujisawa et al. 2018; Sueur, 2006; Xu & Shaw, 2019,
11
12 401 2021). Neutral genetic markers fail to differentiate among such close species, either because
13
14 402 divergence among their songs is too recent for complete lineage sorting or episodes of
15
16 403 introgression on secondary contact have eroded such divergence, or very likely both. Similar
17
18 404 cases of polyphyly among cryptic species of Cicadettini have been detected in *Cicadetta* of
19
20 405 Italy and Greece (Hertach et al., 2015, 2016; Wade et al., 2015), and in *Kikihia* and *Maoricicada*
21
22 406 of New Zealand (Buckley et al. 2006; Marshall et al., 2008), where molecular phylogeny failed
23
24 407 to recover some acoustically defined taxa.

25
26 408 Only a few nuclear genes have been sequenced thus far to investigate phylogenetic
27
28 409 relationships among cicadas worldwide, being EF-1 α the most extensively used and
29
30 410 informative (Arensburger et al., 2004b; Banker et al., 2017; Buckley & Simon, 2007; Hill et al.
31
32 411 2021; Lee & Hill, 2010; Marshal et al., 2008, 2016, 2018; Owen et al., 2017; Price et al., 2019;
33
34 412 Simon et al., 2019). Nuclear genes have been shown as insufficient to resolve the phylogeny of
35
36 413 cryptic cicada species where hybridization is suspected, even when multiple genes were used
37
38 414 (Banker et al., 2017; Buckley & Simon, 2007; Wade et al., 2015). A genomic approach and a
39
40 415 fine-scale sampling at contact zones would be preferable to overcome single-gene
41
42 416 shortcomings and will certainly help to disentangle introgression events and incomplete
43
44 417 lineage sorting among *T. argentata*, *T. mariae* and *T. aneabi*.

45
46 418 Another incongruence between acoustics and genetics found within the *T. helianthemis* ssp.
47
48 419 remains unexplained, as *T. h. galantei* Type II, though sharing the same calling song with *T. h.*
49
50 420 *galantei* Type I, is remarkably different at mitochondrial data. *T. h. galantei* Type II has a
51
52 421 parapatric distribution with Type I (they were not overlapping) with no obvious breaks in
53
54 422 habitat features to justify such level of genetic divergence. Amplification of nuclear
55
56 423 mitochondrial DNA sequences (NUMTs) could be a reason for this pattern of divergence i.e,
57
58 424 mutations at the primer binding sites that would bias amplification towards nuclear copies of
59
60 425 COI at this particular taxon (Song et al., 2008). This seems unlikely since the same phylogenetic
426
427 pattern was recovered for all three independently amplified fragments of mitochondrial DNA
428
429 (COI-LEP, COI-CTL and ATP). Further studies with phylogenomic data should bring some light to
430
431 the roots to this mismatch.

1
2
3
4 4295
6
7 430 **4.2 Biogeographic scenarios**
8

9 431

10
11
12 432 Time estimates inferred with the concatenated model and the multispecies coalescence model
13 433 for the oldest splits within *Tettigettalna* have both very wide confidence intervals (12-2 Ma),
14 434 with which we cannot confidently exclude any of the three scenarios. However, if considering
15 435 mean ages, both methods place the divergence of *T. josei* as a likely pre-MSC or early MSC
16 436 event, probably before the land-bridge was fully established (mean ages of 5.9 and 6.9 Ma,
17 437 respectively). As for the divergence of the Moroccan *T. afroamissa* from the remainder of the
18 438 European *Tettigettalna*, mean age estimates place this event as a likely post-MSC event (4.8
19 439 and 5.3 MA, respectively). Divergence time estimates are sensitive to assumptions used in
20 440 clock calibration, hence a considerable degree of uncertainty is inevitably associated to
21 441 inferred dates (Carruthers & Scotland, 2020), particularly among cicadas, where no accurate
22 442 fossil calibration can be used. When dating divergence events among Cicadettini, Marshall et
23 443 al. (2016) tested many assumptions and attempted to correct inflation when using literature
24 444 based values from other arthropods. Even though relaxed clock models accommodate more
25 445 uncertainty about the substitution rate, configuring analyses such that they adequately
26 446 account for uncertainty remains a challenge (Carruthers & Scotland, 2020).

27
28
29
30
31
32
33
34
35
36
37
38 447 **When** coupling divergence-time estimates with the tree topology, our most parsimonious
39 448 biogeographic reconstruction has a chain of events **scenario** involving three phases (Fig. 6).
40
41 449 First, an ancestral *Tettigettalna* population was likely present across the southern Iberian
42 450 Massif before or during early Messinian (Fig 6A). Then, **in the second phase**, the ancestor of *T.*
43 451 *josei* became geographically or ecologically disconnected from the remainder of the
44 452 *Tettigettalna* in the southwest, where today is southern Portugal (Fig. 6B). This divergence is
45 453 concurrent with the closing of the Baetic and Guadalorce corridors, 7.3 Ma and 6.8 Ma,
46 454 respectively, and the formation of the Guadalquivir Basin (Martin et al., 2001; 2009). Presently
47 455 there is little recorded evidence for the role of the Guadalquivir Sea basin as a biogeographical
48 456 barrier within the Iberian Peninsula, but it has been implied in the divergence of two Iberian
49 457 subspecies of fire salamander, though more recently, during the early Pliocene (Antunes et al.,
50 458 2018; García-París et al., 1998). The progressive uplift of the Baetic basement basin led to the
51 459 formation of the Eurafrikan land connection (Schoorl and Veldkamp, 2003), enabling the main
52
53
54
55
56
57
58
59
60

1
2
3
4 460 *Tettigetta* ancestral population to migrate southwards, into Africa (Fig. 6B). Finally, in the
5
6 461 third phase, the reopening of the Strait of Gibraltar at 5.33 Ma likely worked as an effective
7
8 462 barrier to gene flow between the ancestor of *T. afroamissa* in Africa and “core” *Tettigetta*
9
10 463 in southeastern Iberia (Fig. 6C). Examples of rupture of genetic and biological intercontinental
11
12 464 continuity with the end of MSC are well known among western Mediterranean lineages
13
14 465 occurring in Iberia and/or the Maghreb. To cite only some of the most remarkable, the re-
15
16 466 opening of the Strait of Gibraltar isolated midwife toads *Alytes maurus* from *Alytes dickhilleni*
17
18 467 and *Alytes muletensis* on opposite sides of the Mediterranean (Martínez-Solano et al., 2004),
19
20 468 and the same happened to trapdoor spiders *Ummidia* sp. ‘Tarifa’ and *U. aedificatoria* (Opatova
21
22 469 et al., 2016) and to Anthocharidini butterflies (Marabuto et al., 2020).

23
24 470 The lower 95% HPD for the divergence of *T. afroamissa* points to less than 2.5 Ma, although a
25
26 471 founder event resulting from post-MSC long dispersal to Africa seems very unlikely. Adult
27
28 472 cicadas are short-lived (1-6 weeks) and need to feed daily on plant sap, turning long travelling
29
30 473 overseas without feeding sources on the way into a risky endeavor. Dispersal in cicadas seems
31
32 474 to occur mostly in a step-wise fashion, with travel distances reported as not exceeding 1 km
33
34 475 for large-body *Quesada gigas* (Andrade et al., 2020), 500 m for *Cicada orni* (Simões & Quartau,
35
36 476 2007) or 150 m for *Magicicada* spp. (Karbon, 1981). Even in a scenario where dispersal across
37
38 477 Gibraltar was mediated by extreme winds or other stochastic events (Mas-Peinado et al., 2021;
39
40 478 Osozawa et al., 2021), the likelihood of survival and successful settling afterwards is low. Some
41
42 479 accidental human-mediated introductions of cicada nymphs have been occasionally reported,
43
44 480 likely via potted plants trading (Hertach & Nagel, 2013; Hill et al., 2005; Osozawa et al., 2021;
45
46 481 Pons et al., 2021), but this hypothesis can be safely discarded for *T. afroamissa*, as it was found
47
48 482 in remote and nearly untouched habitats of Morocco (Costa et al., 2017). Adding to this, the
49
50 483 deep level of divergence of *T. afroamissa* from Iberian *Tettigetta* is not compatible with an
51
52 484 anthropogenic founder event.

53
54 485

55 56 486 4.3 The effect of Pleistocene climate changes

57
58 487

59
60 488 After the MSC, with *T. afroamissa* isolated in the Maghreb, and *T. josei* in SW Iberia, the chain
61
62 489 of events therein is however less well supported. Nevertheless, it seems to be closely tied to

1
2
3
4 490 the Pleistocene climate changes, since age estimates inferred with the concatenated model for
5
6 491 species within “core” *Tettigettalna* resulted in upper 95% HPD that do not predate 2.9 Ma,
7
8 492 well after the reopening of the Strait of Gibraltar. Splits are estimated to have occurred in the
9
10 493 early to mid-Pleistocene (Fig 4: nodes F, G, I and J), during the Gelasian and Calabrian periods
11
12 494 (2.58 – 0.781 Ma), coinciding with the acceleration of glacial conditions and the retreat of
13
14 495 populations into more favorable areas, especially the thermophilic ones (Gómez & Lunt, 2007).
15
16 496 Given the heightened species richness of this area, complex geography and climatic stability
17
18 497 over long periods of time (Manzano et al., 2017), it is conceivable that the most recent
19
20 498 common ancestor for most modern *Tettigettalna* could have inhabited the southern portion of
21
22 499 the Iberian Peninsula, and especially the Baetic area. Nowadays, *Tettigettalna* spp. in southern
23
24 500 Iberia have parapatric or partially overlapping distributions and it is likely that finer-scale
25
26 501 sampling would detect hybrid zones between sister taxa, as detected for Cicadettini cicadas of
27
28 502 the genus *Kikihia* (Marshall et al., 2008, 2011; Banker et al., 2017). The genus *Kikihia* provides a
29
30 503 remarkable example of species-rich lineages that experienced rapid evolutionary radiation of
31
32 504 song-defined cryptic species during the Pleistocene, as mountain-building isolated populations
33
34 505 and affected habitat structure in New Zealand (Marshall et al., 2008; Marshall et al., 2011).
35
36 506 This process might be analogous to what could have happened with *Tettigettalna* in southern
37
38 507 Iberia, at a smaller geographical scale.

39
40 508 Among extant Iberian “core” *Tettigettalna*, only *T. estrellae* seems not to be affiliated with the
41
42 509 Baetic southern hotspot of diversity. Instead, the NW Iberian distribution of *T. estrellae* seems
43
44 510 to gravitate around a putative glacial refugium represented by the Douro valley or mountains
45
46 511 around it, as seen for other ectotherms such as newts (Martínez-Solano et al., 2006), lizards
47
48 512 (Miraldo et al. 2011; Paulo et al., 2001) and vipers (Martínez-Freiría et al., 2020). Likewise, the
49
50 513 northern clade of widespread *T. argentata* probably expanded from some uncertain refugia,
51
52 514 up and beyond the Iberian Peninsula. Haplotypes found in France and Italy seem to be the
53
54 515 most derived, but further sampling and genomic data is necessary to investigate the
55
56 516 phylogeography of *T. argentata* in its full range. We found no consistent differences in ecology
57
58 517 or morphology compared to other *Tettigettalna* spp. that could explain *T. argentata*'s success
59
60 518 in expanding northwards (Mendes et al., 2014; Puissant & Sueur, 2010; Nunes et al., 2014b).
519
520 519 Perhaps tolerance to temperate climate, adaptation to a wider range of plant hosts or less
521
522 520 competition with other *Tettigettalna* while expanding from southern refugia could be
523
524 521 hypotheses to explore in the future.

1
2
3
4 522 Several other cicada species share a similar trans-Mediterranean distribution as *Tettigettna*.
5
6 523 Genera such as *Cicada*, *Tibicina*, *Euryphara* or *Pseudotettigettna* have species on both sides of
7
8 524 the Strait of Gibraltar, but the North-African counterparts remain poorly studied (Pinto-Juma
9
10 525 et al, 2009; Puissant & Sueur, 2010; Sueur et al, 2007). We hope that future studies may lessen
11
12 526 the knowledge gap between the two continents and investigate the underlying causes for their
13
14 527 current patterns of distribution.
15
16 528

17 18 529 **Credit authorship contribution statement**

19
20 530 Study design: GJC, VLN, OSP, PCS; Sampling: VLN, EM, RM, PP, JMB, TH; DNA isolation and
21
22 531 sequencing: VLN; Data analyses: GJC, VLN, DNS; Writing: GJC, VLN. All authors contributed to
23
24 532 review the final manuscript.
25

26 534 **Acknowledgements**

27
28
29 535 The authors wish to thank Francisco Pina-Martins, Ana S. Rodrigues, Ana Vieira and Sara Ema
30
31 536 Silva for discussing results, troubleshooting and image design. We thank Chris Simon for
32
33 537 reviewing the manuscript.
34

35 538 36 37 38 539 **Funding**

39
40 540 This work was financially supported by the project PTDC/ BIA-BIC/115511/2009 from the
41
42 541 Portuguese Foundation for Science and Technology (FCT). Fieldwork was funded by a grant
43
44 542 from the Systematics Research Fund awarded to Paula C. Simões in 2014 by the Royal Linnean
45
46 543 Society and the Systematics Association.
47

48 544 49 50 51 545 **Declaration of Competing Interest**

52
53 546 The authors declare that they have no known competing financial interests or personal
54
55 547 relationships that could have appeared to influence the work reported in this paper.
56
57

58 548
59
60

1
2
3
4 549 **Supplemental material**

5
6 550

7
8 551 **Figure S1.** Single locus Bayesian trees for mitochondrial loci.

9
10 552 **Figure S2.** Single locus Maximum likelihood trees for mitochondrial loci.

11
12 553 **Figure S3.** Maximum likelihood tree for concatenated mitochondrial loci.

13
14 554 **Figure S4.** Maximum likelihood tree for the nuclear locus EF1- α .

15
16 555

17
18 556 **Table S1.** Specimens included in phylogenetic analyses, with collection points, codes, GPS
19 557 coordinates and GenBank accession numbers.

20
21 558 **Table S2.** Primers and annealing temperature used to amplify each locus.

22
23 559 **SuppInfo_beast_input.xml** input file used for BEAST analysis.

24
25 560 **SuppInfo_star_beast_input.xml** input file used for *BEAST analysis.

26
27 561

28
29 562

30
31
32 563 **5. BIBLIOGRAPHY**

33
34
35 564 Andrade, S.C., Rossi, G.D., & Martinelli, N.M. (2020). Dispersion pattern of Giant Cicada
36 565 (Hemiptera: Cicadidae) in a Brazilian coffee plantation. *Environmental Entomology*, 49, 1019–
37 566 1025. <https://doi.org/10.1093/ee/nvaa096>

38
39
40 567 Antunes, B., Lourenço, A., Caeiro-Dias, G. M., Dinis, H., Gonçalves, I., Martínez-Solano, P. &
41 568 Velo-Anton, G. (2018) Combining phylogeography and landscape genetics to infer the
42 569 evolutionary history of a short-range Mediterranean relict, *Salamandra salamandra*
43 570 *longirostris*. *Conservation Genetics*, 19, 1411–1424. [https://doi.org/10.1007/s10592-018-1110-](https://doi.org/10.1007/s10592-018-1110-7)

44
45 571 7

46
47
48
49 572 Arensburger, P., Simon, C., & Holsinger, K. (2004a). Evolution and phylogeny of the New
50 573 Zealand cicada genus *Kikihia* Dugdale (Homoptera: Auchenorrhyncha: Cicadidae) with special
51 574 reference to the origin of the Kermadec and Norfolk Islands' species. *Journal of Biogeography*,
52 575 31, 1769–1783. <https://doi.org/10.1111/j.1365-2699.2004.01098.x>

53
54
55 576 Arensburger, P. Buckley, T. R., Simon, C., Moulds, M. & Holsinger, K.E. (2004b). Biogeography
56 577 and phylogeny of the New Zealand cicada genera (Hemiptera: Cicadidae) based on nuclear and
57
58
59
60

- 1
2
3
4 578 mitochondrial DNA data. *Journal of Biogeography*, 31, 557-569.
5
6 579 <https://doi.org/10.1046/j.1365-2699.2003.01012.x>
7
8 580 Ballard, J. W. O. & Whitlock, M. C. (2004). The incomplete natural history of mitochondria.
9
10 581 *Molecular Ecology*, 13, 729-744. <https://doi.org/10.1046/j.1365-294X.2003.02063.x>
11
12 582 Banker, S. E., Elizabeth, J. W., Simon, C. (2017). The confounding effects of hybridization on
13
14 583 phylogenetic estimation in the New Zealand cicada genus *Kikihia*. *Molecular Phylogenetics and*
15
16 584 *Evolution*, 116, 172-181. <https://doi.org/10.1016/j.ympev.2017.08.009>.
17
18 585 Boulard, M. (2006). Acoustic signals, diversity and behaviour of cicadas (Cicadidae, Hemiptera).
19
20 586 In: *Insect Sounds and Communication* (eds Drosopoulos S & Claridge MF), pp. 331–349. CRC
21
22 587 Press, Florida, USA.
23
24 588 Bator, J., Marshall, D. C., Hill, K. B., Cooley, J. R., Leston, A., & Simon, C. (2022). Phylogeography
25
26 589 of the endemic red-tailed cicadas of New Zealand (Hemiptera: Cicadidae: *Rhodopsalta*), and
27
28 590 molecular, morphological and bioacoustical confirmation of the existence of Hudson's
29
30 591 *Rhodopsalta microdora*. *Zoological Journal of the Linnean Society*, 195, 1219-1244.
31
32 592 <https://doi.org/10.1093/zoolinnean/zlab065>
33
34 593 Blanc, P. (2002). The opening of the Plio-Quaternary Gibraltar Strait: assessing the size of a
35
36 594 cataclysm. *Geodinamica Acta*, 15, 303–317. [https://doi.org/10.1016/S0985-3111\(02\)01095-1](https://doi.org/10.1016/S0985-3111(02)01095-1)
37
38 595 Buckley, T. R. & Simon, C. (2007). Evolutionary radiation of the cicada genus *Maoricicada*
39
40 596 Dugdale (Hemiptera: Cicadoidea) and the origins of the New Zealand alpine biota. *Biological*
41
42 597 *Journal of the Linnean Society*, 91, 419–435. [https://doi.org/10.1111/j.1095-](https://doi.org/10.1111/j.1095-8312.2007.00807.x)
43
44 598 [8312.2007.00807.x](https://doi.org/10.1111/j.1095-8312.2007.00807.x)
45
46 599 Buckley, T. R., Cordeiro, M., Marshall, D. C. & Simon, C. (2006). Differentiating between
47
48 600 hypotheses of lineage sorting and introgression in New Zealand alpine cicadas (*Maoricicada*
49
50 601 Dugdale). *Systematic Biology*, 55, 411–425, <https://doi.org/10.1080/10635150600697283>
51
52 602 Carruthers, T., Scotland, R. W. (2020). Uncertainty in divergence time estimation. *Systematic*
53
54 603 *Biology*, 70, 855–861, <https://doi.org/10.1093/sysbio/syaa096>
55
56 604 Costa, G. J., Nunes, V. L., Marabuto, E., Mendes, R., Laurentino, T. G., Quartau, J. A., Paulo, O.
57
58 605 S. & Simões, P. (2017). Morphology, songs and genetics identify two new cicada species from
59
60 606 Morocco: *Tettigettna afroamissa* sp. nov. and *Berberigettna dimelodica* gen. nov. & sp. nov.

- 1
2
3
4 607 (Hemiptera: Cicadettini). *Zootaxa*, 4237, 517. <https://doi.org/10.11646/zootaxa.4237.3.4>
- 5
6
7 608 Drummond, A. J., Suchard, M. A., Xie, D. & Rambaut, A. (2012). Bayesian phylogenetics with
8
9 609 BEAUti and the BEAST 1.7. *Molecular Biology and Evolution*, 29, 1969–1973.
10
11 610 <https://doi.org/10.1093/molbev/mss075>
- 12 611 Dumitru, O. A., Austermann, J., Polyak, V.J., Fornós, J.J., Asmerom, Y., Ginés, J., ... Onac, B.P.
13
14 612 (2021). Sea-level stands from the Western Mediterranean over the past 6.5 million years.
15
16 613 *Scientific Reports*, 11, 261. <https://doi.org/10.1038/s41598-020-80025-6>
- 17
18 614 Elez, J., Silva, P. G., Huerta, P., Perucha, M. Á., Civis, J., Roquero, E., ... Martínez-Graña, A.
19
20 615 (2016). Quantitative paleotopography and paleogeography around the Gibraltar Arc (South
21
22 616 Spain) during the Messinian Salinity Crisis. *Geomorphology*, 275, 26–45.
23
24 617 <https://doi.org/10.1016/j.geomorph.2016.09.023>
- 25 618 Feliner, G. N. (2011). Southern European glacial refugia: A tale of tales. *Taxon*, 60, 365–372.
26
27 619 <https://doi.org/10.1002/tax.602007>
- 28
29 620 Flot, J.-F., Tillier, A., Samadi, S. & Tillier, S. (2006). Phase determination from direct sequencing
30
31 621 of length-variable DNA regions. *Molecular Ecology Notes*, 6, 627–630.
32
33 622 <https://doi.org/10.1111/j.1471-8286.2006.01355.x>
- 34 623 García-Aloy, S., Vitales, D., Roquet C., Sanmartín, I., Vargas, P., Molero, J., ... Alarcón, M.
35
36 624 (2017). North-west Africa as a source and refuge area of plant biodiversity: a case study on
37
38 625 *Campanula kremeri* and *Campanula occidentalis*. *Journal of Biogeography*, 44, 2057-2068.
39
40 626 <https://doi.org/10.1111/jbi.12997>
- 41
42 627 Fujisawa, T., Koyama, T., Kakishima, S., Cooley, J. R., Simon, C., Yoshimura, J. & Sota, T. (2018).
43
44 628 Triplicate parallel life cycle divergence despite gene flow in periodical cicadas. *Communications*
45
46 629 *Biology*, 1, 26. <https://doi.org/10.1038/s42003-018-0025-7>
- 47
48 630 García-París, M., Alcobendas, M., Alberch, P. & Garcia-Paris, M. (1998). Influence of the
49
50 631 Guadalquivir river basin on mitochondrial DNA evolution of *Salamandra salamandra* (Caudata:
51
52 632 Salamandridae) from Southern Spain. *Copeia*, 1998, 173-176.
53
54 633 <https://doi.org/10.2307/1447714>
- 55
56 634 Gibert, L., Scott, G. R., Montoya, P., Ruiz-Sánchez, F. J., Morales, J., Luque, L., ... Lería, M.
57
58 635 (2013). Evidence for an African-Iberian mammal dispersal during the pre-evaporitic Messinian.
59
60

- 1
2
3
4 636 Geology, 41, 691–694. <https://doi.org/10.1130/G34164.1>
5
6
7 637 Gogala, M. & Gogala, A. (1999). A checklist and provisional atlas of the Cicadoidea fauna of
8
9 638 Slovenia (Homoptera: Auchenorrhyncha). Acta Entomologica Slovenica, 7, 119–128.
10
11 639 Gómez, A. & Lunt, D. H. (2007). Refugia within refugia: Patterns of phylogeographic
12
13 640 concordance in the Iberian Peninsula, in: Phylogeography of Southern European Refugia.
14
15 641 Springer Netherlands, Dordrecht, pp. 155–188. https://doi.org/10.1007/1-4020-4904-8_5
16
17 642 Habel, J.C., Lens, L., Rödder, D. & Schmitt, T. (2011). From Africa to Europe and back: refugia
18
19 643 and range shifts cause high genetic differentiation in the Marbled White butterfly *Melanargia*
20
21 644 *galathea*. BMC Evolutionary Biology, 11, 215. <https://doi.org/10.1186/1471-2148-11-215>
22
23 645 Heled, J., Bouckaert, R., Drummond, A. J. & Xie, W. (2013). *BEAST in BEAST 2.0 Estimating
24
25 646 Species Trees from Multilocus Data 1–18.
26
27 647 Heled, J. & Drummond, A. J. (2010). Bayesian inference of species trees from multilocus data.
28
29 648 Molecular Biology and Evolution, 27, 570–580. <https://doi.org/10.1093/molbev/msp274>
30
31 649 Hertach, T. & Nagel, P. (2013). Cicadas in Switzerland: A scientific overview of the historic and
32
33 650 current knowledge of a popular taxon (Hemiptera: Cicadidae). Revue Suisse de Zoologie, 120,
34
35 651 229–269.
36
37 652 Hertach, T., Puissant, S., Gogala, M., Trilar, T., Hagmann, R., Baur, H., ... Nagel, P. (2016).
38
39 653 Complex within a complex: Integrative taxonomy reveals hidden diversity in *Cicadetta*
40
41 654 *brevipennis* (Hemiptera: Cicadidae) and unexpected relationships with a song divergent
42
43 655 relative. PLoS One 11, e0165562. <https://doi.org/10.1371/journal.pone.0165562>
44
45 656 Hertach, T., Trilar, T., Wade, E. J., Simon, C. & Nagel, P. (2015). Songs, genetics, and
46
47 657 morphology: revealing the taxonomic units in the European *Cicadetta cerdaniensis* cicada
48
49 658 group, with a description of new taxa (Hemiptera: Cicadidae). Zoological Journal of the Linnean
50
51 659 Society, 173, 320-351. <https://doi.org/10.1111/zoj.12212>
52
53 660 Hewitt, G. (2000). The genetic legacy of the Quaternary ice ages. Nature, 405, 907–913.
54
55 661 <https://doi.org/10.1038/35016000>
56
57 662 Hewitt, G. M. (1999). Post-glacial re-colonization of European biota. Biological Journal of the
58
59 663 Linnean Society, 68, 87–112. <https://doi.org/10.1111/j.1095-8312.1999.tb01160.x>
60

- 1
2
3
4 664 Hill, K. B., Marshall, D. C., & Cooley, J. R. (2005). Crossing Cook Strait: possible human
5 665 transportation and establishment of two New Zealand cicadas from North Island to South
6 666 Island (*Kikihia scutellaris* and *K. ochrina*, Hemiptera: Cicadidae). *New Zealand Entomologist*, 28,
7 667 71-80. <https://doi.org/10.1080/00779962.2005.9722688>
8
9
10
11
12 668 Hill, K. B. R., Marshall, D. C., Marathe, K., Moulds, M. S., Lee, Y. J., ... & Simon, C. (2021). The
13 669 molecular systematics and diversification of a taxonomically unstable group of Asian cicada
14 670 tribes related to *Cicadini* Latreille, 1802 (Hemiptera : Cicadidae). *Invertebrate Systematics*, 35,
15 671 570-601. <https://doi.org/10.1071/IS20079>
16
17
18
19
20 672 Husemann, M., Schmitt, T., Zachos, F. E., Ulrich, W. & Habel, J. C. (2014). Palaeartic
21 673 biogeography revisited: Evidence for the existence of a North African refugium for Western
22 674 Palaeartic biota. *Journal of Biogeography*, 41, 81–94. <https://doi.org/10.1111/jbi.12180>
23
24
25
26 675 Jolivet, L., Augier, R., Robin, C., Suc, J. P. & Rouchy, J. M. (2006). Lithospheric-scale geodynamic
27 676 context of the Messinian salinity crisis. *Sedimentary Geology*, 188–189, 9–33.
28 677 <https://doi.org/10.1016/j.sedgeo.2006.02.004>
29
30
31
32 678 Karban, R. (1981). Flight and dispersal of periodical cicadas. *Oecologia*, 49, 385–390.
33 679 <https://doi.org/10.1007/BF00347604>
34
35
36
37 680 Katoh, K. & Standley, D. M. (2013). MAFFT Multiple Sequence Alignment Software Version 7:
38 681 Improvements in Performance and Usability. *Molecular Biology and Evolution*, 30, 772–780.
39 682 <https://doi.org/10.1093/molbev/mst010>
40
41
42 683 Knowles, L.L., Chappell, T. M., Marquez, E. J. & Cohn, T. J.(2016). Tests of the role of sexual
43 684 selection in genitalic divergence with multiple hybrid clines. *Journal of Orthoptera Research*,
44 685 25, 75-82.
45
46
47
48 686 Krijgsman, W., Capella, W., Simon, D., Hilgen, F. J., Kouwenhoven, T. J., Meijer, P. T., ... ,
49 687 Flecker, R. (2018). The Gibraltar Corridor: Watergate of the Messinian Salinity Crisis. *Marine*
50 688 *Geology*, 403, 238–246. <https://doi.org/10.1016/j.margeo.2018.06.008>
51
52
53
54 689 Krijgsman, W., Hilgen, F. J., Raffi, I., Sierro, F. J. & Wilson, D. S. (1999). Chronology, causes and
55 690 progression of the Messinian salinity crisis. *Nature*, 400, 652–655.
56 691 <https://doi.org/10.1038/23231>
57
58
59
60

- 1
2
3
4 692 Lambert, S. M., Reeder, T. W. & Wiens, J. J. (2015). When do species-tree and concatenated
5 693 estimates disagree? An empirical analysis with higher-level scincid lizard phylogeny. *Molecular*
6 694 *Phylogenetics and Evolution*, 82, 146–155. <https://doi.org/10.1016/j.ympev.2014.10.004>
9
10 695 Langerhans, R. B., Anderson, C. M. & Heinen-Kay, J. L.(2016). Causes and consequences of
11 696 genital evolution. *Integrative and Comparative Biology*, 56, 741–751.
12 697 <https://doi.org/10.1093/icb/icw101>
13
14 698 Lanfear, R., Frandsen, P. B., Wright, A. M., Senfeld, T. & Calcott, B. (2016). PartitionFinder 2:
15 699 New methods for selecting partitioned models of evolution for molecular and morphological
16 700 phylogenetic analyses. *Molecular Biology and Evolution*, 34, 772–773.
17 701 <https://doi.org/10.1093/molbev/msw260>
18
19 702 Lanier, H. C. & Knowles, L. L. (2015). Applying species-tree analyses to deep phylogenetic
20 703 histories: Challenges and potential suggested from a survey of empirical phylogenetic studies.
21 704 *Molecular Phylogenetics and Evolution*, 83, 191–199.
22 705 <https://doi.org/10.1016/j.ympev.2014.10.022>
23
24 706 Lavergne, S., Hampe, A. & Arroyo, J. (2013). In and out of Africa: how did the Strait of Gibraltar
25 707 affect plant species migration and local diversification? *Journal of Biogeography*, 40, 24–36.
26 708 <https://doi.org/10.1111/j.1365-2699.2012.02769.x>
27
28 709 Lee, Y. J. & Hill, K. B. R. (2010) Systematic revision of the genus *Psithyristria* Stal (Hemiptera:
29 710 Cicadidae) with seven new species and a molecular phylogeny of the genus and higher taxa.
30 711 *Systematic Entomology*, 35, 277–305. <https://doi.org/10.1111/j.1365-3113.2009.00509.x>
31
32 712 Librado, P. & Rozas, J. (2009). DnaSP v5: a software for comprehensive analysis of DNA
33 713 polymorphism data. *Bioinformatics*, 25, 1451–1452.
34 714 <https://doi.org/10.1093/bioinformatics/btp187>
35
36 715 Manzano, S., Carrión, J. S., López-Merino, L., González-Sampériz, P., Munuera, M., Fernández,
37 716 S., ... Ferreras, M. del C. (2017). Mountain strongholds for woody angiosperms during the Late
38 717 Pleistocene in SE Iberia. *CATENA*, 149, 701–712. <https://doi.org/10.1016/j.catena.2016.03.008>
39
40 718 Manzi, V., Gennari, R., Hilgen, F., Krijgsman, W., Lugli, S., Roveri, M. & Sierro, F. J. (2013). Age
41 719 refinement of the Messinian salinity crisis onset in the Mediterranean. *Terra Nova*, 25, 315–
42 720 322. <https://doi.org/10.1111/ter.12038>
43
44
45
46
47
48
49
50
51
52
53
54
55
56
57
58
59
60

- 1
2
3
4 721 Marabuto, E., Pina-Martins, F., Rebelo, M. T. & Paulo, O. S. (2020). Ancient divergence, a crisis
5
6 722 of salt and another of ice shaped the evolution of the west Mediterranean butterfly *Euchloe*
7
8 723 *tagis*. *Biological Journal of the Linnean Society*, 131, 487–504.
9
10 724 <https://doi.org/10.1093/biolinnean/blaa129>
11
12 725 Marshall, D. C., Hill, K. B. R., Cooley, J. R. & Simon, C. (2011). Hybridization, mitochondrial DNA
13
14 726 phylogeography, and prediction of the early stages of reproductive isolation: Lessons from
15
16 727 New Zealand cicadas (Genus *Kikihia*). *Systematic Biology*, 60, 482–502.
17
18 728 <https://doi.org/10.1093/sysbio/syr017>
19
20 729 Marshall, D. C., Hill, K. B. R., Moulds, M., Vanderpool, D., Cooley, J. R., Mohagan, A.B. & Simon,
21
22 730 C. (2016). Inflation of molecular clock rates and dates: Molecular phylogenetics, biogeography,
23
24 731 and diversification of a global cicada radiation from Australasia (Hemiptera: Cicadidae:
25
26 732 Cicadettini). *Systematic Biology*, 65, 16–34. <https://doi.org/10.1093/sysbio/syv069>
27
28 733 Marshall, D. C., Moulds, M., Hill, K. B. R., Price, B. W., Wade, E. J., Owen, C. L., ... Simon, C.
29
30 734 (2018). A molecular phylogeny of the cicadas (Hemiptera: Cicadidae) with a review of tribe and
31
32 735 subfamily classification. *Zootaxa*, 4424, 1-64. doi: 10.11646/zootaxa.4424.1.1. PMID:
33
34 736 30313477.
35
36 737 Marshall, D. C., Slon, K., Cooley, J. R., Hill, K. B. R. & Simon, C. (2008). Steady Plio-Pleistocene
37
38 738 diversification and a 2-million-year sympatry threshold in a New Zealand cicada radiation.
39
40 739 *Molecular Phylogenetics and Evolution*, 48, 1054–1066.
41
42 740 <https://doi.org/10.1016/j.ympev.2008.05.007>
43
44 741 Martín, J. M., Braga, J. C., Aguirre, J. & Puga-Bernabéu, Á. (2009). History and evolution of the
45
46 742 North-Betic Strait (Prebetic Zone, Betic Cordillera): A narrow, early Tortonian, tidal-dominated,
47
48 743 Atlantic-Mediterranean marine passage. *Sedimentary Geology*, 216, 80–90.
49
50 744 <https://doi.org/10.1016/j.sedgeo.2009.01.005>
51
52 745 Martin, J. M., Braga, J. C. & Betzler, C. (2001). The messinian Guadalquivir corridor: The last
53
54 746 Northern, atlantic-mediterranean gateway. *Terra Nova*, 13, 418–424.
55
56 747 <https://doi.org/10.1046/j.1365-3121.2001.00376.x>
57
58 748 Martínez-Freiría, F., Freitas, I., Zuffi, M. A. L., Golay, P., Ursenbacher, S. & Velo-Antón, G.
59
60 749 (2020). Climatic refugia boosted allopatric diversification in Western Mediterranean vipers.
750 *Journal of Biogeography*, 1–16. <https://doi.org/10.1111/jbi.13861>

- 1
2
3
4 751 Martínez-Solano, I., Gonçalves, H. A., Arntzen, J. W., García-París, M. (2004). Phylogenetic
5 752 relationships and biogeography of midwife toads (Discoglossidae: *Alytes*). *Journal of*
6 753 *Biogeography*, 31, 603–618. <https://doi.org/doi:10.1046/j.1365-2699.2003.01033.x>
7
8
9
10 754 Martínez-Solano, I., Teixeira, J., Buckley, D. & García-París, M. (2006). Mitochondrial DNA
11 755 phylogeography of *Lissotriton boscai* (Caudata, Salamandridae): evidence for old, multiple
12 756 refugia in an Iberian endemic. *Molecular Ecology*, 15, 3375–3388.
13 757 <https://doi.org/10.1111/j.1365-294X.2006.03013.x>
14
15 758 Mas-Peinado, P., García-París, M., Ruiz, J. L. & Buckley, D. (2021). The Strait of Gibraltar is an
16 759 ineffective palaeogeographic barrier for some flightless darkling beetles (Coleoptera:
17 760 Tenebrionidae: *Pimelia*), *Zoological Journal of the Linnean Society*, zlab088,
18 761 <https://doi.org/10.1093/zoolinnean/zlab088>
19
20
21
22
23
24 762 McCormack, J. E., Heled, J., Delaney, K. S., Peterson, A. T. & Knowles, L. L. (2010). Calibrating
25 763 divergence times on species trees versus gene trees: implications for speciation history of
26 764 *Aphelocoma* jays. *Evolution*, 65, 184–202. <https://doi.org/10.1111/j.1558-5646.2010.01097.x>
27
28
29
30 765 Médail, F. & Diadema, K. (2009). Glacial refugia influence plant diversity patterns in the
31 766 Mediterranean Basin. *Journal of Biogeography*, 36, 1333–1345.
32 767 <https://doi.org/10.1111/j.1365-2699.2008.02051.x>
33
34 768 Mendes, J, Harris, D. J., Carranza, S., Salvi, D. (2007). Biogeographical crossroad across the
35 769 Pillars of Hercules: Evolutionary history of *Psammadromus* lizards in space and time. *Journal of*
36 770 *Biogeography*, 44, 2877–2890. <https://doi.org/10.1111/jbi.13100>
37
38
39
40
41 771 Mendes, R., Nunes, V. L., Quartau, J. A. & Simões, P. C. (2014). Patterns of acoustic and
42 772 morphometric variation in species of genus *Tettigetta* (Hemiptera: Cicadidae): Sympatric
43 773 populations show unexpected differences. *European Journal of Entomology*, 111, 429–441.
44 774 <https://doi.org/10.14411/eje.2014.054>
45
46
47
48
49 775 Miller, M.A., Pfeiffer, W. & Schwartz, T. (2010). Creating the CIPRES Science Gateway for
50 776 inference of large phylogenetic trees, in: 2010 Gateway Computing Environments Workshop
51 777 (GCE). IEEE, pp. 1–8. <https://doi.org/10.1109/GCE.2010.5676129>
52
53 778 Miraldo, A., Hewitt, G. M., Paulo, O. S. & Emerson, B. C. (2011). Phylogeography and
54 779 demographic history of *Lacerta lepida* in the Iberian Peninsula: multiple refugia, range
55
56
57
58
59
60

- 1
2
3
4 780 expansions and secondary contact zones. *BMC Evolutionary Biology*, 11, 170.
5
6 781 <https://doi.org/10.1186/1471-2148-11-170>
7
8
9 782 Moulds, M. S. (2018). Cicada fossils (Cicadoidea: Tettigarctidae and Cicadidae) with a review of
10 783 the named fossilised Cicadidae. *Zootaxa*, 4438, 443-470. doi: 10.11646/zootaxa.4438.3.2.
11
12 784 PMID: 30313130.
13
14
15 785 Nunes, V., Mendes, R., Quartau, J. A. & Simões, P. C. (2014b). Current distribution raises
16 786 concerns on the conservation of *Tettigettna mariae* (Quartau & Boulard, 1995) (Hemiptera:
17 787 Cicadoidea) in Portugal. *Ecologi@*, 7, 50–57.
18
19
20
21 788 Nunes, V.L., Mendes, R., Marabuto, E., Novais, B.M., Hertach, T., Quartau, J.A., ... Simões, P.C.
22 789 (2014a). Conflicting patterns of DNA barcoding and taxonomy in the cicada genus *Tettigettna*
23 790 from southern Europe (Hemiptera: Cicadidae). *Molecular Ecology and Resources*, 14, 27–38.
24 791 <https://doi.org/10.1111/1755-0998.12158>
25
26
27
28
29 792 Opatova, V., Bond, J. E. & Arnedo, M. A. (2016). Uncovering the role of the Western
30 793 Mediterranean tectonics in shaping the diversity and distribution of the trap-door spider genus
31 794 *Ummidia* (Araneae, Ctenizidae). *Journal of Biogeography*, 43, 1955–1966.
32 795 <https://doi.org/10.1111/jbi.12838>
33
34
35
36 796 Osozawa, S., Kanai, K., Fukuda, H. & Wakabayashi, J. (2021). Phylogeography of Ryukyu insular
37 797 cicadas: Extensive vicariance by island isolation vs accidental dispersal by super typhoon. *PLoS*
38 798 *One*, 16, e0244342. <https://doi.org/10.1371/journal.pone.0244342>
39
40
41
42
43 799 Owen, C. L., Marshall, D. C., Kathy, B. R. H., Simon, C. (2017). How the aridification of Australia
44 800 structured the biogeography and influenced the diversification of a large lineage of Australian
45 801 cicadas. *Systematic Biology*, 66, 569–589. <https://doi.org/10.1093/sysbio/syw078>
46
47
48
49 802 Paulo, O. S., Dias, C., Bruford, M. W., Jordan, W. C. & Nichols, R. A. (2001). The persistence of
50 803 Pliocene populations through the Pleistocene climatic cycles: evidence from the
51 804 phylogeography of an Iberian lizard. *Proceedings of the Royal Society of London. Series B*
52 805 *Biological Sciences*, 268, 1625–1630. <https://doi.org/10.1098/rspb.2001.1706>
53
54
55
56 806 Paulo, O. S., Pinheiro, J., Miraldo, A., Bruford, M. W., Jordan, W. C. & Nichols, R. A. (2008). The
57 807 role of vicariance vs. dispersal in shaping genetic patterns in ocellated lizard species in the
58
59
60

- 1
2
3
4 808 western Mediterranean. *Molecular Ecology*, 17, 1535–1551. <https://doi.org/10.1111/j.1365->
5 294X.2008.03706.x
6 809
7
8 810 Petit, R. J. (2003). Glacial refugia: Hotspots but not melting pots of genetic diversity. *Science*,
9 300, 1563–1565. <https://doi.org/10.1126/science.1083264>
10 811
11
12 812 Pinto-Juma, G. A., Quartau, J. A. & Bruford, M. W. (2009). Mitochondrial DNA variation and the
13 evolutionary history of the Mediterranean species of *Cicada*. L. (Hemiptera, Cicadoidea).
14 *Zoological Journal of the Linnean Society*, 155, 266–288, <https://doi.org/10.1111/j.1096->
15 3642.2008.00437.x
16 814
17 815
18
19
20 816 Pons, P., Font, R. C., Franch, M., Bas, J. M., Fraga, D. E., Fontelles, F. & Franch, M.(2021).
21 Diversitat, distribució i fenologia de les cigales (Hemiptera: Cicadidae) a Catalunya (NE
22 Península Iberica). *Bulletí de la Institució Catalana d'Història Natural*, 85, 59-72.
23 817
24 818
25
26 819 Price, B. W., Marshall, D. C., Barker, N. P., Simon, C. & Villet, M. H. (2019). Out of Africa? A
27 dated molecular phylogeny of the cicada tribe Platycleurini Schmidt (Hemiptera: Cicadidae),
28 with a focus on African genera and the genus *Platycleura* Amyot & Audinet-Serville. *Systematic*
29 *Entomology*, 44, 842-861. <https://doi.org/10.1111/syen.12360>
30 820
31 821
32 822
33
34 823 Puissant, S. & Sueur, J. (2010). A hotspot for Mediterranean cicadas (Insecta: Hemiptera:
35 Cicadidae): new genera, species and songs from southern Spain. *Systematics and Biodiversity*,
36 8, 555–574. <https://doi.org/10.1080/14772000.2010.532832>
37 824
38 825
39
40 826 Rodrigues, A. S. B., Silva, S. E., Marabuto, E., Silva, D. N., Wilson, M. R., Thompson, V., ...
41 Seabra, S. G. (2014). New mitochondrial and nuclear evidences support recent demographic
42 expansion and an atypical phylogeographic pattern in the spittlebug *Philaenus spumarius*
43 (Hemiptera, Aphrophoridae). *PLoS One*, 9, e98375.
44 828
45 829
46 830
47 831
48 832
49 833
50 834
51 835
52 836
53 837
54 838
55 839
56 840
57 841
58 842
59 843
60 844

- 1
2
3
4 836 large model space. *Systematic Biology*, 61, 539–542. <https://doi.org/10.1093/sysbio/sys029>
5
6
7 837 Rubinoff, D. & Holland, B. S. (2005). Between Two Extremes: Mitochondrial DNA is neither the
8
9 838 Panacea nor the Nemesis of Phylogenetic and Taxonomic Inference. *Systematic Biology*, 54,
10 839 952–961. <https://doi.org/10.1080/10635150500234674>
11
12
13 840 Sanborn, A. F. (2014). *Catalogue of the Cicadoidea (Hemiptera: Auchenorrhyncha)*. Academic
14 841 Press, San Diego, California.
15
16
17 842 Schmitt, T. (2007). Molecular biogeography of Europe: Pleistocene cycles and postglacial
18 843 trends. *Frontiers in Zoology*, 4, 1–13. <https://doi.org/10.1186/1742-9994-4-11>
19
20
21 844 Schoorl, J. M. & Veldkamp, A. (2003). Late Cenozoic landscape development and its tectonic
22 845 implications for the Guadalhorce valley near Álora (Southern Spain). *Geomorphology*, 50, 43–
23 846 57. [https://doi.org/10.1016/S0169-555X\(02\)00207-6](https://doi.org/10.1016/S0169-555X(02)00207-6)
24
25
26
27 847 Shaw, K. L. (2002). Conflict between nuclear and mitochondrial DNA phylogenies of a recent
28 848 species radiation: what mtDNA reveals and conceals about modes of speciation in Hawaiian
29 849 crickets. *Proceedings of the National Academy of Sciences*, 99, 16122-16127.
30 850 <https://doi.org/10.1073/pnas.242585899>
31
32
33
34
35 851 Simões, P. C., Nunes, V. L., Mendes, R., Seabra, S. G. & Paulo, O. S. (2014). *Tettigetta josei*
36 852 (Boulard, 1982) (Hemiptera: Cicadoidea): first record in Spain, with notes on the distribution,
37 853 genetic variation and behaviour of the species. *Biodiversity Data Journal*, 2.
38 854 <https://doi.org/10.3897/BDJ.2.e1045>
39
40
41
42
43 855 Simões, P. C. & Quartau, J. A. (2007). On the dispersal of males of *Cicada orni* in Portugal
44 856 (Hemiptera: Cicadidae). *Entomologia Generalis*, 30, 245–252.
45
46
47
48 857 Simon, C., Cooley, J. R., Karban, R., & Sota, T. (2022). Advances in the evolution and ecology of
49 858 13- and 17-year periodical cicadas. *Annual Review of Entomology*, 67, 457-482.
50 859 <https://doi.org/10.1146/annurev-ento-072121-061108>
51
52
53 860 Simon, C., Gordon, E. R. L., Moulds, M. S., Cole, J. A., Haji, D., Lemmon, A. R., ... Piotr Łukasik,
54 861 (2019). Off-target capture data, endosymbiont genes and morphology reveal a relict lineage
55 862 that is sister to all other singing cicadas. *Biological Journal of the Linnean Society*, 128, 865–
56 863 886, <https://doi.org/10.1093/biolinnean/blz120>
57
58
59
60

- 1
2
3
4 864 Song, H., Buhay, J. E., Whiting, M. F. & Crandall, K. A. (2008). Many species in one: DNA
5 865 barcoding overestimates the number of species when nuclear mitochondrial pseudogenes are
6 866 coamplified. *Proceedings of the National Academy of Sciences*, 105, 13486–13491.
7
8 867 <https://doi.org/10.1073/pnas.0803076105>
9
10
11
12 868 Stamatakis, A. (2014). RAxML version 8: A tool for phylogenetic analysis and post-analysis of
13 869 large phylogenies. *Bioinformatics* 30, 1312–1313.
14
15 870 <https://doi.org/10.1093/bioinformatics/btu033>
16
17
18 871 Stephens, M., Smith, N. J. & Donnelly, P. (2001). A new statistical method for haplotype
19 872 reconstruction from population data. *American Journal of Human Genetics*, 68, 978–989.
20
21 873 <https://doi.org/10.1086/319501>
22
23 874 Sueur, J. (2006). Insect species and their songs. In: *Insect Sounds and Communication* (eds
24 875 Drosopoulos S & Claridge MF), pp. 331–349. CRC Press, Florida, USA.
26
27
28 876 Sueur, J., Vanderpool, D., Simon, C., Ouvrard, D. & Bourgoïn, T. (2007). Molecular phylogeny of
29 877 the genus *Tibicina* (Hemiptera, Cicadidae): rapid radiation and acoustic behavior. *Biological*
30 878 *Journal of the Linnean Society*, 91, 611–626, [https://doi.org/10.1111/j.1095-](https://doi.org/10.1111/j.1095-8312.2007.00823.x)
31 879 [8312.2007.00823.x](https://doi.org/10.1111/j.1095-8312.2007.00823.x)
32
33
34
35 880 Trájer, A. J., Sebestyén, V., Padisák, J. (2021) The impacts of the Messinian Salinity Crisis on
36 881 the biogeography of three Mediterranean sandfly (Diptera: Psychodidae) species. *Geobios*, 65,
37 882 51-66. <https://doi.org/10.1016/j.geobios.2021.02.003>
38
39
40
41 883 Tonini, J., Moore, A., Stern, D., Shcheglovitova, M. & Ortí, G. (2015). Concatenation and species
42 884 tree methods exhibit statistically indistinguishable accuracy under a range of simulated
43 885 conditions. *PLoS Currents*, 7.
44
45 886 <https://doi.org/10.1371/currents.tol.34260cc27551a527b124ec5f6334b6be>
46
47
48
49 887 Tzedakis, P. C. (2009). Museums and cradles of Mediterranean biodiversity. *Journal of*
50 888 *Biogeography*, 36, 1033–1034. <https://doi.org/10.1111/j.1365-2699.2009.02123.x>
51
52 889 Veith, M., Mayer, C., Samraoui, B., Barroso, D. D. & Bogaerts, S. (2004) From Europe to Africa
53 890 and vice versa: evidence for multiple intercontinental dispersal in ribbed salamanders (Genus
54 891 *Pleurodeles*). *Journal of Biogeography*, 31, 159–171. [https://doi.org/10.1111/j.1365-](https://doi.org/10.1111/j.1365-2699.2004.00957.x)
55 892 [2699.2004.00957.x](https://doi.org/10.1111/j.1365-2699.2004.00957.x)
56
57
58
59
60

- 1
2
3
4 893 Wade, E. J., Hertach, T., Gogala, M., Trilar, T. & Simon, C. (2015). Molecular species
5 894 delimitation methods recover most song-delimited cicada species in the European *Cicadetta*
6 895 *montana* complex. *Journal of Evolutionary Biology*, 28, 2318–2336.
7 896 <https://doi.org/10.1111/jeb.12756>
- 8 897 Xia, X. & Xie, Z. (2001). DAMBE: Software package for data analysis in molecular biology and
9 898 evolution. *Journal of Heredity*, 92, 371–373. <https://doi.org/10.1093/jhered/92.4.371>
- 10 899 Xia, X., Xie, Z., Salemi, M., Chen, L. & Wang, Y. (2003). An index of substitution saturation and
11 900 its application. *Molecular Phylogenetics and Evolution*, 26, 1–7.
12 901 [https://doi.org/10.1016/S1055-7903\(02\)00326-3](https://doi.org/10.1016/S1055-7903(02)00326-3)
- 13 902 Xu, M. & Shaw, K. L. (2019). The genetics of mating song evolution underlying rapid speciation:
14 903 linking quantitative variation to candidate genes for behavioral isolation. *Genetics*, 211, 1089–
15 904 1104, <https://doi.org/10.1534/genetics.118.301706>
- 16 905 Xu, M. & Shaw, K. L. (2021). Extensive linkage and genetic coupling of song and preference loci
17 906 underlying rapid speciation in *Laupala* crickets. *Journal of Heredity*, 112, 204–213,
18 907 <https://doi.org/10.1093/jhered/esab001>

908 909 **Legends of figures**

910 **Figure 1.** Major geological events of the Western Mediterranean, Pleistocenic glacial refugia
911 and *Tettigettalna* spp. distributions. Panels A – D show a schematic of the evolution of the
912 West Mediterranean region from the Tortonian to the Late Pleistocene. A – Mid Tortonian,
913 depicting the three Eurafriean corridors that later closed, between 7.8 to 6.0 Ma. B – Late
914 Messinian, during the Salinity Crisis an extensive land bridge formed between Iberia and North
915 Africa. Arrow points to the Guadalquivir basin, a large saltwater basin. C – Early Pliocene, land
916 bridge is now disrupted, and the Guadalquivir basin has almost retreated. D – Late Pleistocene,
917 during the period when sea level was the lowest, according to Rohling et al. (2014), approx.
918 150 m lower. No land bridges are present during this period. Putative Pleistocenic glacial
919 refugia of the Western Mediterranean inferred for flora (Médail & Diadema 2009) in green,
920 and terrestrial fauna and flora (Gómez & Lunt 2007) shown with broken lines. E – Present day
921 *Tettigettalna* spp. distributions in orange, according to Puissant & Sueur (2010), Simões et al.,

1
2
3
4 922 (2014), Nunes et al. (2014b) and Costa *et al.* (2017). Legend: 1–*T. estrellae*; 2–*T. josei*; 3–*T.*
5 923 *mariae*; 4–*T. armandi*; 5–*T. aneabi*; 6–*T. defaulti*; 7– *T. helianthemi helianthemi*; 8–*T. h.*
6 924 *galantei*; 9–*T. boulandi*; 10–*T. afroamissa*. Species' distributions in brown overlap with those of
7
8 925 other species. The distribution of *T. argentata* is not shown as it is widespread across several
9
10 926 European countries and the Iberian Peninsula with exception of the Baetic ranges in
11
12 927 southeastern Iberia. Scale bar equals 100 km.

13
14
15 928 **Figure 2.** Sampling of *Tettigettalna* spp. Circles indicate same-species collection points. Due to
16
17 929 the volume of sampling from the Southern Iberian Peninsula, the smaller box below shows
18
19 930 additional sampling points for other species annotated for that area. Legend: 1–*T. estrellae*; 2–
20
21 931 *T. josei*; 3–*T. mariae*; 4–*T. armandi*; 5–*T. aneabi*; 6–*T. defaulti*; 7– *T. helianthemi helianthemi*;
22
23 932 8–*T. h. galantei*; 9–*T. boulandi*; 10–*T. afroamissa*; 11A –*T. argentata* South Clade; 11B – *T.*
24
25 933 *argentata* North Clade; 11C – *T. argentata* Central Clade; 11D – *T. argentata* Catalonia Clade.

26
27 934 **Figure 3.** Bayesian phylogenetic trees for the concatenated mitochondrial loci (A) and nuclear
28
29 935 EF-1 α (b). Posterior probabilities > 0.90 are shown next to branch nodes. Scale bar represents
30
31 936 the number of estimated changes per branch length. *H. varipes* (Hva608), *C. barbara* (Cba203)
32
33 937 and *C. orni* (Cor298) were set as outgroup. Root length was truncated for imaging purposes.

34
35 938 **Figure 4.** *Tettigettalna* species tree with concatenation model as output of BEAST. Posterior
36
37 939 probabilities >0.9 are shown next to each node. Node bars A-J illustrate the 95% HPD interval
38
39 940 (age estimates for each node are listed in Table 2). **Vertical gray shading** under the timescale
40
41 941 bar refers to two past geological events: the Messinian Salinity Crisis and the Pleistocene Ice
42
43 942 ages. To illustrate song diversity within the target genus, oscillograms are shown next to each
44
45 943 taxon.

46
47 944 **Figure 5.** Age estimate boxplots of the possible nodes by the multispecies coalescent species-
48
49 945 tree with *BEAST. The first boxplot plots the age estimates of the basal node of *Tettigettalna*,
50
51 946 with the remainder plotting a different topology (TAF=*T. afroamissa*, TJO= *T. josei*, TCO= "core"
52
53 947 *Tettigettalna*).

54
55 948 **Figure 6.** DensiTree output of the Bayesian inference species tree of *Tettigettalna* with the
56
57 949 partitioned unlinked mtCOI and nuEF-1 α dataset. The consensus trees are shown by the bold
58
59 950 blue line. Uncertainty of node heights and topology is shown by the transparent green, purple
60
951 and red lines. Core *Tettigettalna* refers to the clade composed of the remainder of the

1
2
3
4 952 *Tettigettalna* (see methods for explanation). Scale bar indicates Ma. The broken lines A-C refer
5
6 953 to key moments in time illustrated in the left panes. A) Mid-Tortonian (~10-8 Ma) when the
7
8 954 ancestral population of the *Tettigettalna* occurred in the southern Iberian Peninsula; the
9
10 955 broken line marks the separation of the *T. josei* lineage from the main ancestral population. B)
11
12 956 Late Messinian, during the Salinity Crisis, when the main population disperses to North Africa,
13
14 957 via the formed land bridge; the broken line indicates the rupture caused by the opening of the
15
16 958 Gibraltar Strait by end of the Messinian (5.33 Ma). C) Early Pliocene (~4 Ma), showing the three
17
18 959 lineages: *T. josei* in Southwestern Iberia; *T. afroamissa* in Morocco and the remainder of the
19
20 960 European *Tettigettalna* lineage which would later diverge into all other species. In the lower
21
22 961 left corner, a female of the Moroccan species *T. afroamissa* is shown.
23
24
25 962
26
27 963

27 **Table 1.** Loci sequenced for *Tettigettalna*, with information about sequence length, number of
28 individuals sequenced (N), number of haplotypes, number of variable sites (V) and number of
29 parsimony-informative sites (P).
30
31 964

Locus name	Locus Size (bp)	N	Haplotypes	V	P
COI-Lep mtDNA	581	148	83	208	175
COI-CTL mtDNA	683	59	41	106	76
ATP mtDNA	668	55	42	211	162
EF-1 α nuDNA	561	63	59*	82*	30

32
33
34
35
36
37
38
39
40
41
42 965 *including indels
43
44 966
45
46 967
47
48 968
49
50 969
51
52 970
53
54 971
55
56 972
57
58 973
59
60

974

975 **Table 2.** Mean age estimates in million years ago (Ma) and 95% highest posterior density (HPD)
 976 intervals for nodes A to J, as in Fig. 4, according to BEAST analysis (concatenation model).

977

Node	Mean \pm Std Error	95% HPD Interval
A	5.9191 \pm 9.18x10 ⁻³	2.8488 - 9.6307
B	4.8203 \pm 7.48x10 ⁻³	2.2826 - 7.8374
C	3.4142 \pm 5.26x10 ⁻³	1.6048 - 5.5004
D	2.7216 \pm 4.21x10 ⁻³	1.3082 - 4.4336
E	2.5574 \pm 4.00x10 ⁻³	1.2458 - 4.1976
F	1.8258 \pm 2.84x10 ⁻³	0.8167 - 2.9201
G	1.2287 \pm 2.15x10 ⁻³	0.4944 - 2.1052
H	2.9220 \pm 4.60x10 ⁻³	1.3616 - 4.7695
I	1.5040 \pm 2.43x10 ⁻³	0.6722 - 2.5244
J	1.2858 \pm 2.05x10 ⁻³	0.5653 - 2.0989

978

979

980

981 **Table 3.** Mean age estimates in million years ago (Ma) and 95% highest probability density
 982 intervals of tMRCA as in Fig.5 according to *BEAST analysis (multispecies coalescent model).
 983 Clade support is given in percentage of trees post-burnin that support that topology.

984

Split	Mean \pm Std Error	95% HPD Interval	Support
<i>Tettigettalna spp</i>	7.039 \pm 0.080	2.638 -12.274	95.12%
<i>T. afroamissa</i> / <i>T. josei</i>	6.952 \pm 0.080	2.429x10 ⁻³ - 12.41	9.00%
<i>T. afroamissa</i> / "Core" <i>Tettigettalna</i>	5.308 \pm 0.054	2.047 - 9.565	81.59%
<i>T. josei</i> / "Core" <i>Tettigettalna</i>	6.965 \pm 0.080	2.548 - 12.297	8.40%

985

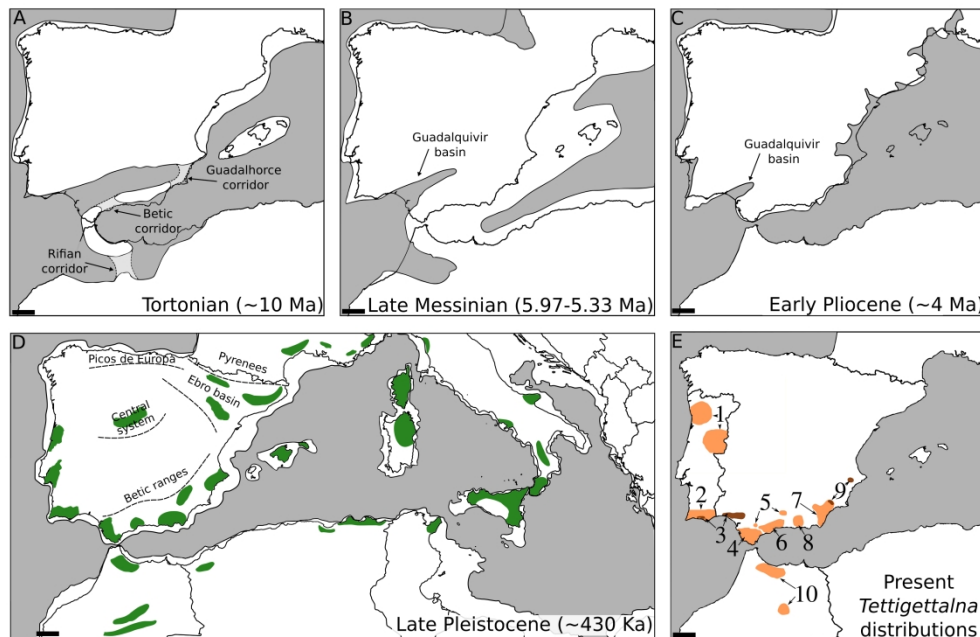


Figure 1. Major geological events of the Western Mediterranean, Pleistocenic glacial refugia and *Tettigettna* spp. distributions. Panels A – D show a schematic of the evolution of the West Mediterranean region from the Tortonian to the Late Pleistocene. A – Mid Tortonian, depicting the three Eurafrican corridors that later closed, between 7.8 to 6.0 Ma. B – Late Messinian, during the Salinity Crisis an extensive land bridge formed between Iberia and North Africa. Arrow points to the Guadalquivir basin, a large saltwater basin. C – Early Pliocene, land bridge is now disrupted, and the Guadalquivir basin has almost retreated. D – Late Pleistocene, during the period when sea level was lowest, according to Rohling et al. (2014), approx. 150 m lower. No land bridges are present during this period. Putative Pleistocenic glacial refugia of the Western Mediterranean inferred for flora (Médail & Diadema 2009) in green, and terrestrial fauna and flora (Gómez & Lunt 2007) shown with broken lines. E – Present day *Tettigettna* spp. distributions in orange, according to Puissant & Sueur (2010), Simões et al., (2014), Nunes et al. (2014b) and Costa et al. (2017). Legend: 1–*T. estrellae*; 2–*T. josei*; 3–*T. mariae*; 4–*T. armandi*; 5–*T. aneabi*; 6–*T. defaulti*; 7–*T. helianthemi helianthemi*; 8–*T. h. galantei*; 9–*T. bouldardi*; 10–*T. afroamissa*. Species' distributions in brown overlap with those of other species. The distribution of *T. argentata* is not shown as it is widespread across several European countries and the Iberian Peninsula with exception of the Baetic ranges in southeastern Iberia. Scale bar equals 100 km.

755x499mm (118 x 118 DPI)

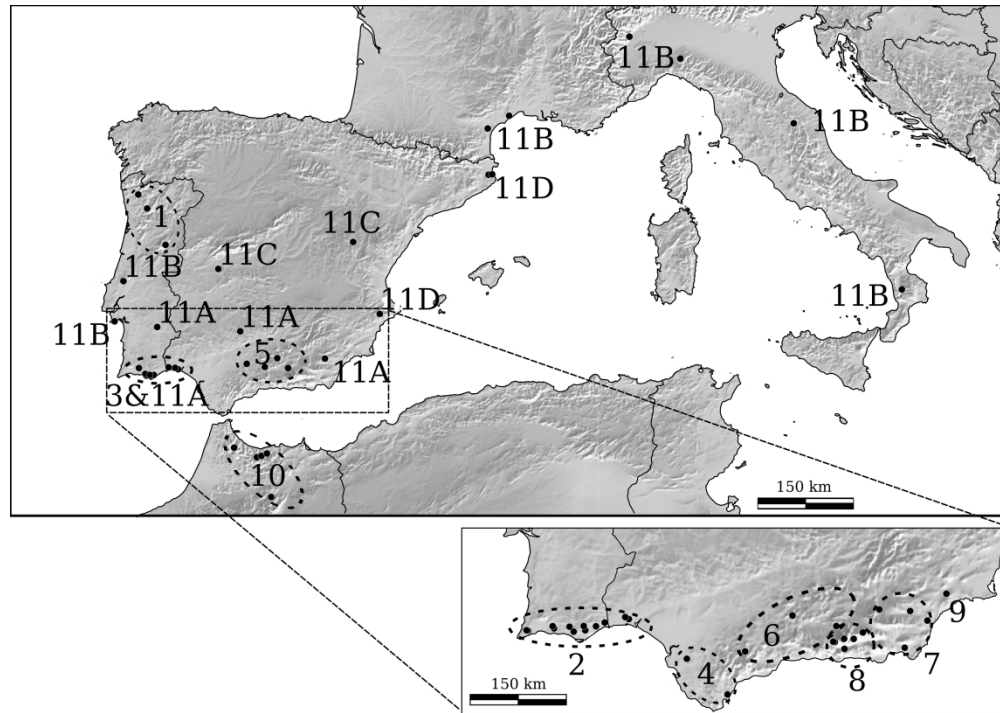
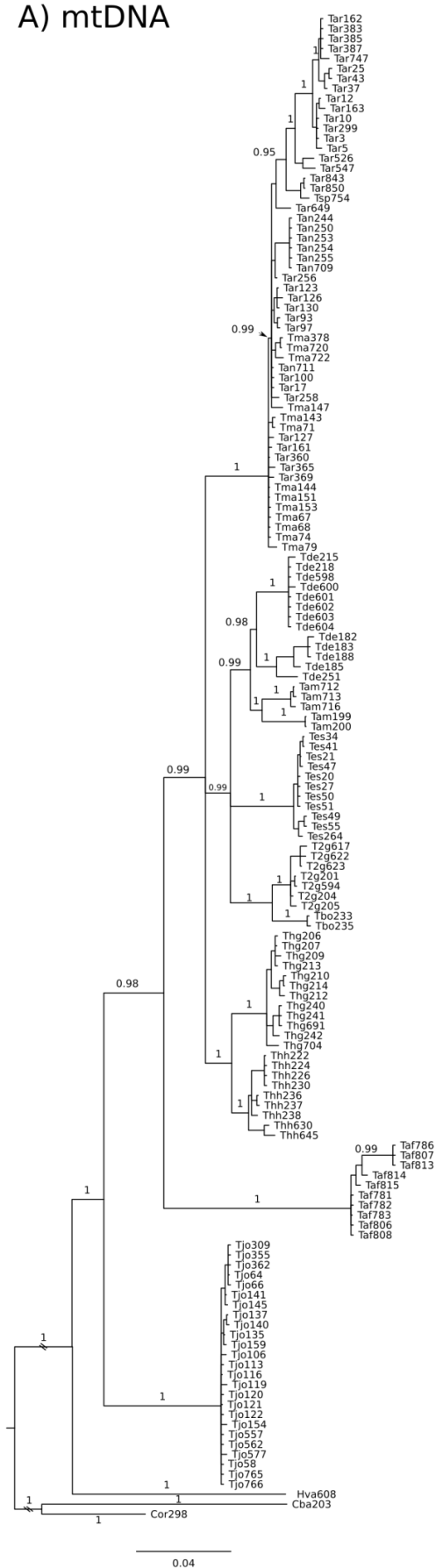


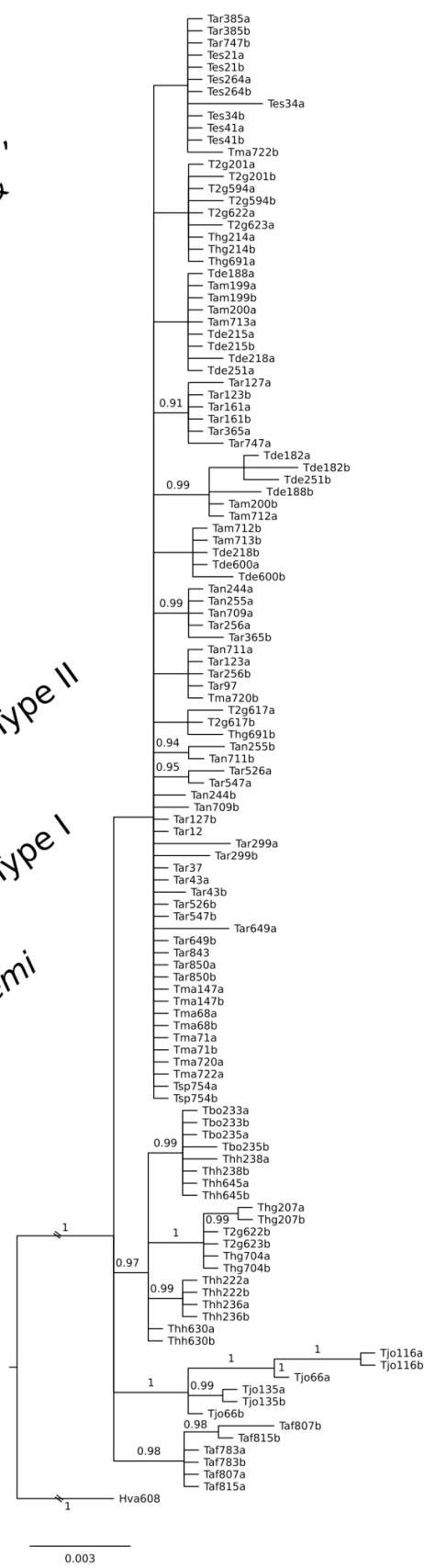
Figure 2. Sampling of *Tettigettalna* spp. Circles indicate same-species collection points. Due to the volume of sampling from the Southern Iberian Peninsula, the smaller box below shows additional sampling points for other species annotated for that area. Legend: 1-*T. estrellae*; 2-*T. josei*; 3-*T. mariae*; 4-*T. armandi*; 5-*T. aneabi*; 6-*T. defauti*; 7- *T. helianthemis helianthemis*; 8-*T. h. galantei*; 9-*T. bouldardi*; 10-*T. afroamissa*; 11A -*T. argentata* South Clade; 11B - *T. argentata* North Clade; 11C - *T. argentata* Central Clade; 11D - *T. argentata* Catalonia Clade.

731x518mm (118 x 118 DPI)

A) mtDNA



B) EF-1α



T. argentata,
T. mariae &
T. aneabi

T. defauti

T. armandi

T. estrellae

T. h. galantei Type II

T. boulandi

T. h. galantei Type I

T. h. helianthemi

T. afroamissa

T. josei

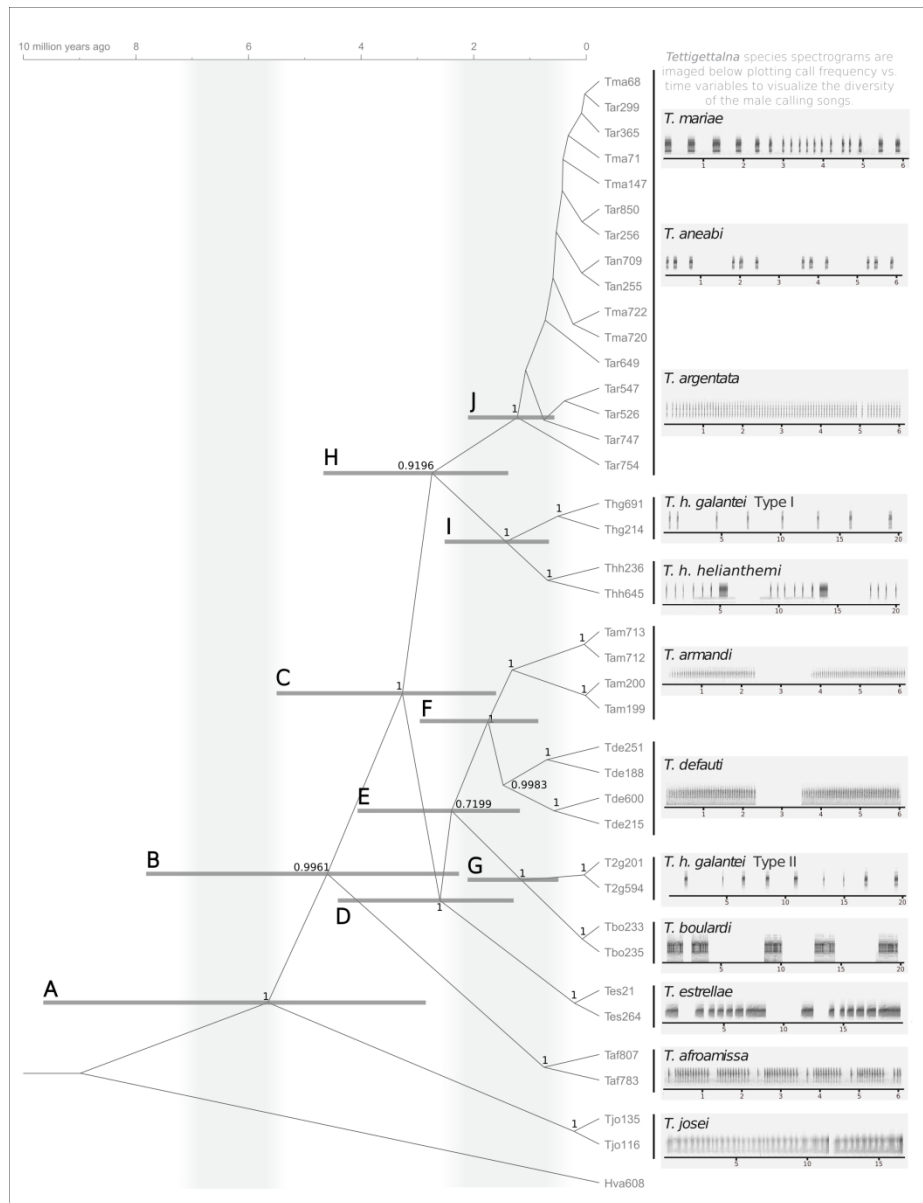


Figure 4. *Tettigettalna* species tree with concatenation model as output of BEAST. Posterior probabilities >0.9 are shown next to each node. Node bars A-J illustrate the 95% HPD interval (age estimates for each node are listed in Table 2). Vertical gray shading under the timescale bar refers to two past geological events: the Messinian Salinity Crisis and the Pleistocene Ice ages. To illustrate song diversity within the target genus, oscillograms are shown next to each taxon.

542x699mm (118 x 118 DPI)

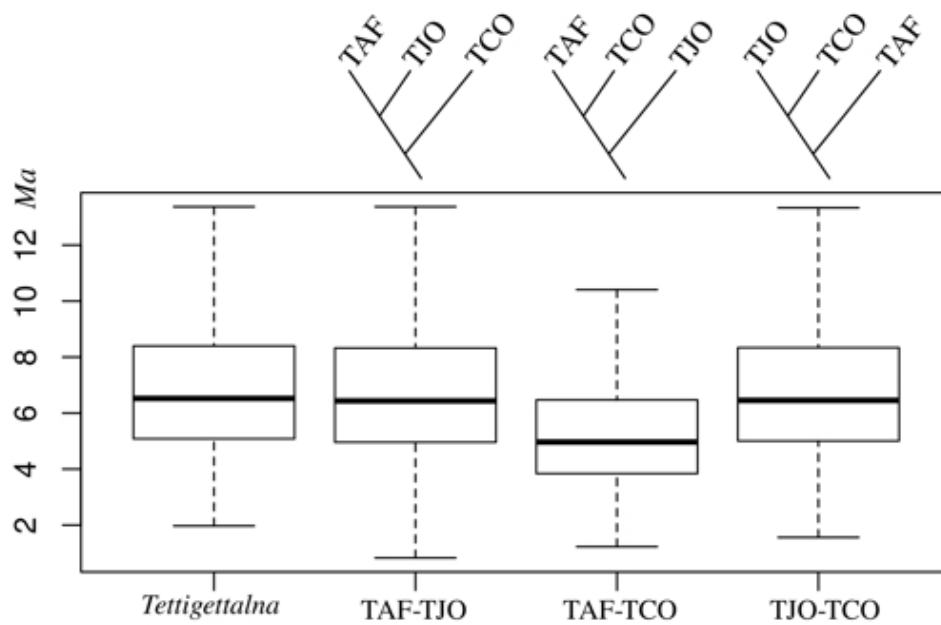


Figure 5. Age estimate boxplots of the possible nodes by the multispecies coalescent species-tree with *BEAST. The first boxplot plots the age estimates of the basal node of *Tettigettalna*, with the remainder plotting a different topology (TAF=*T. afroamissa*, TJO= *T. josei*, TCO= "core" *Tettigettalna*).

185x126mm (72 x 72 DPI)

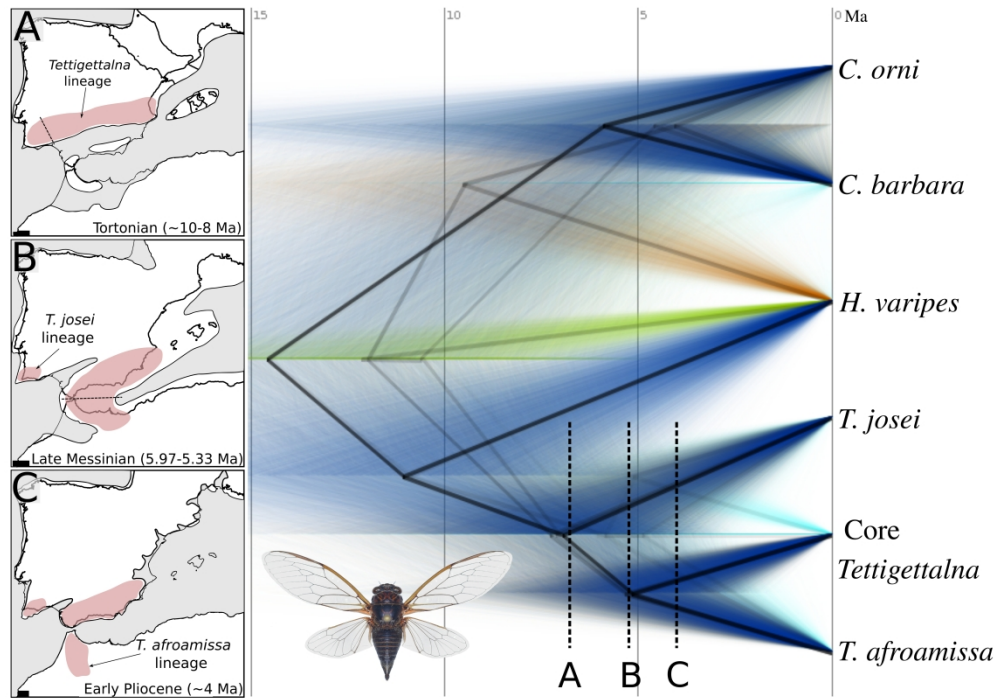


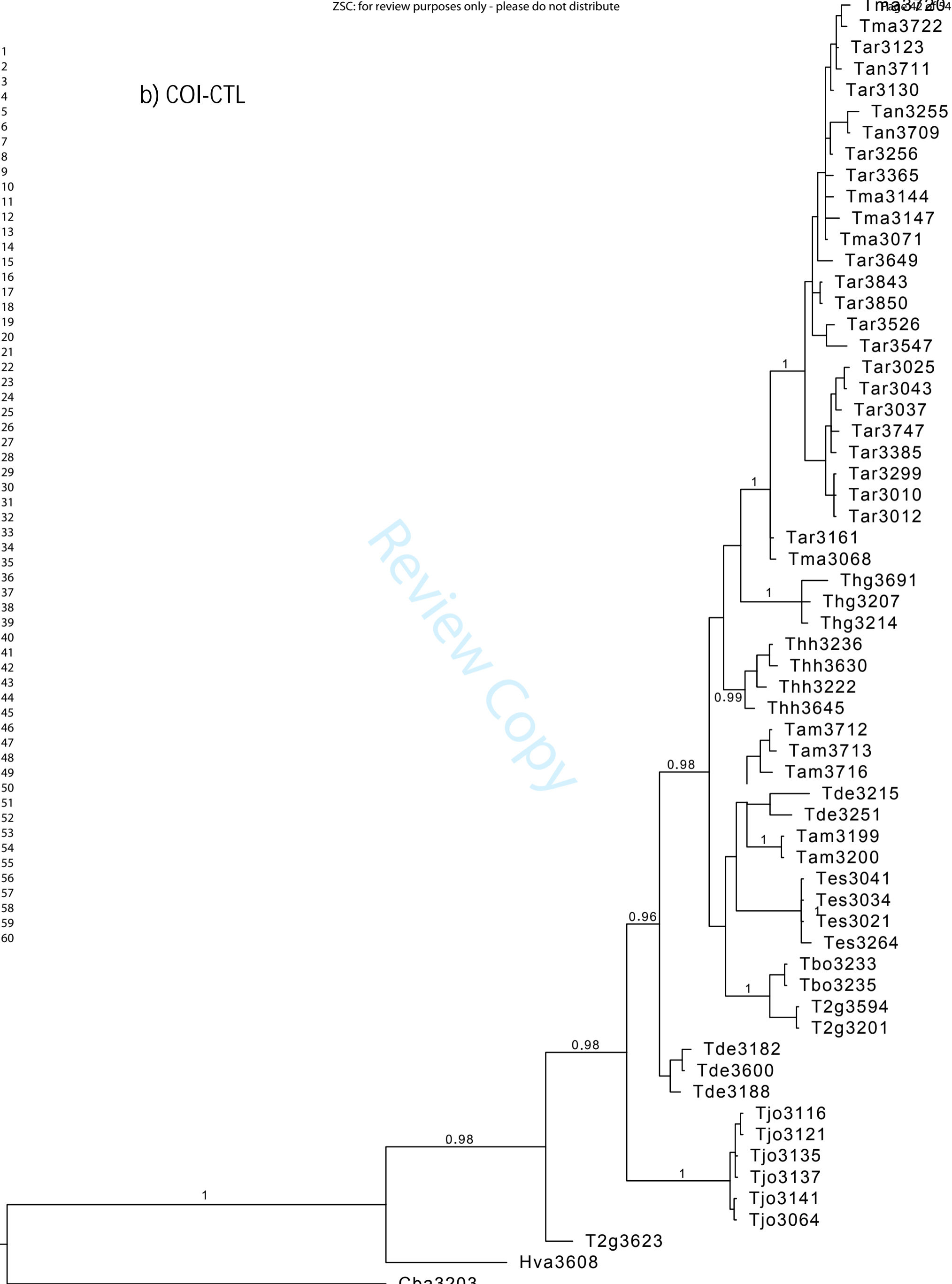
Figure 6. DensiTree output of the Bayesian inference species tree of *Tettigetta* with the partitioned unlinked mtCOI and nuEF-1 α dataset. The consensus trees are shown by the bold blue line. Uncertainty of node heights and topology is shown by the transparent green, purple and red lines. Core *Tettigetta* refers to the clade composed of the remainder of the *Tettigetta* (see methods for explanation). Scale bar indicates Ma. The broken lines A-C refer to key moments in time illustrated in the left panes. A) Mid-Tortonian (\sim 10-8 Ma) when the ancestral population of the *Tettigetta* occurred in the southern Iberian Peninsula; the broken line marks the separation of the *T. josei* lineage from the main ancestral population. B) Late Messinian, during the Salinity Crisis, when the main population disperses to North Africa, via the formed land bridge; the broken line indicates the rupture caused by the opening of the Gibraltar Strait by end of the Messinian (5.33 Ma). C) Early Pliocene (\sim 4 Ma), showing the three lineages: *T. josei* in Southwestern Iberia; *T. afroamissa* in Morocco and the remainder of the European *Tettigetta* lineage which would later diverge into all other species. In the lower left corner, a female of the Moroccan species *T. afroamissa* is shown.

623x438mm (236 x 236 DPI)

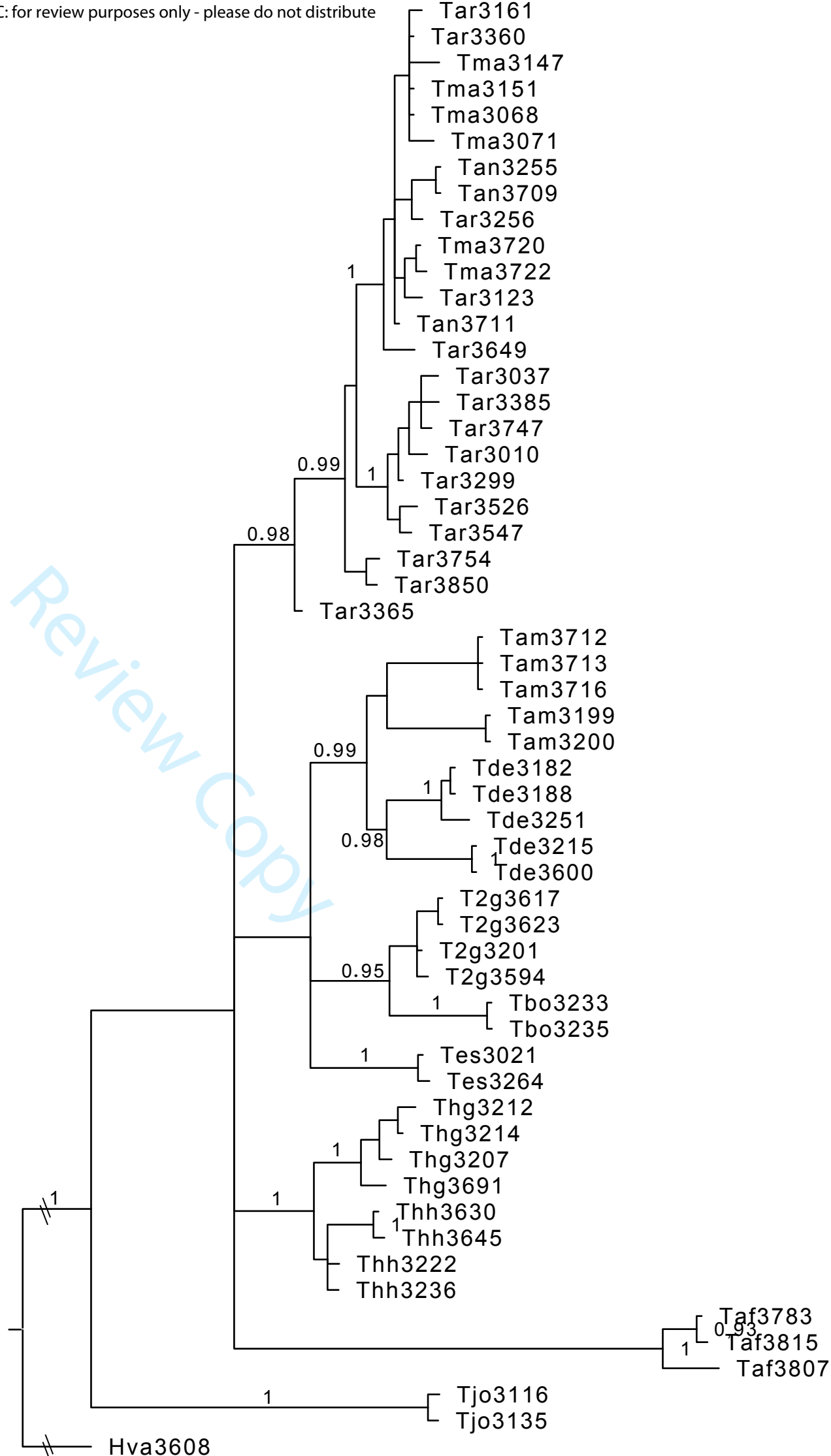
b) COI-CTL

1
2
3
4
5
6
7
8
9
10
11
12
13
14
15
16
17
18
19
20
21
22
23
24
25
26
27
28
29
30
31
32
33
34
35
36
37
38
39
40
41
42
43
44
45
46
47
48
49
50
51
52
53
54
55
56
57
58
59
60

Review Copy



c) ATP



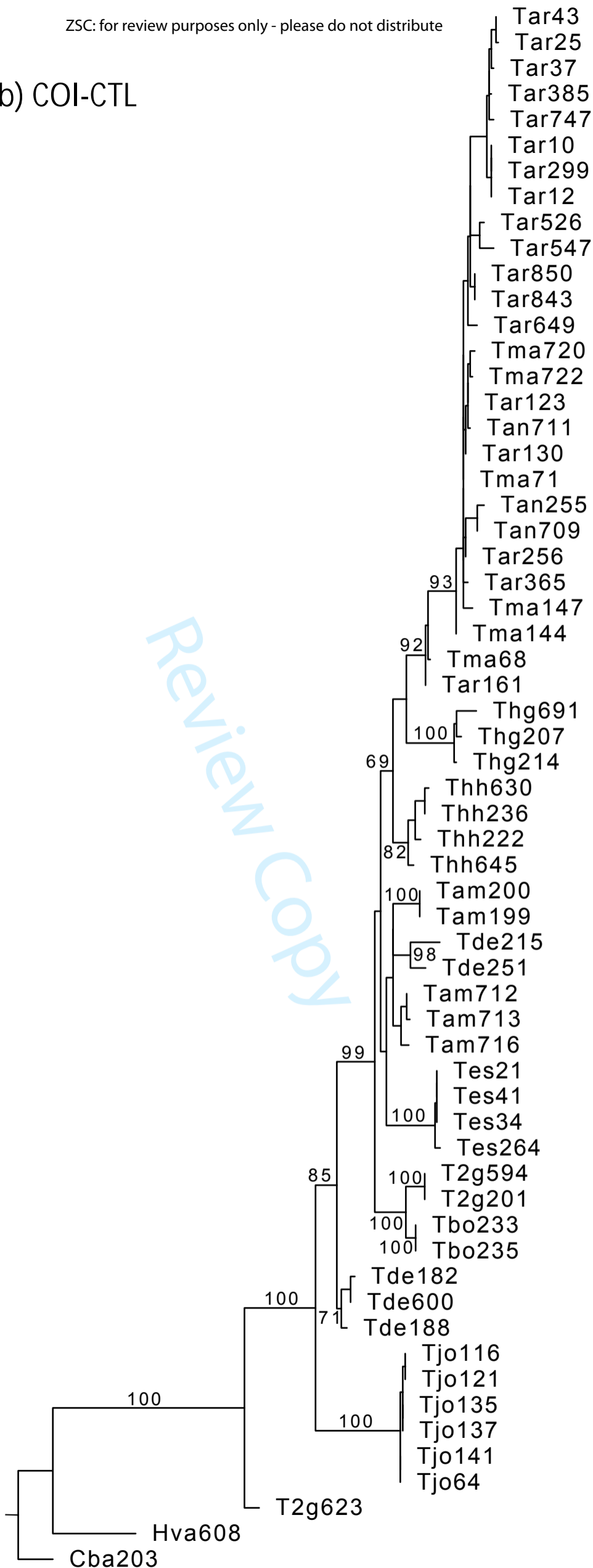
ZSC submitted manuscript

0.03

1
2
3
4
5
6
7
8
9
10
11
12
13
14
15
16
17
18
19
20
21
22
23
24
25
26
27
28
29
30
31
32
33
34
35
36
37
38
39
40
41
42
43
44
45
46
47
48
49
50
51
52
53
54
55
56
57
58
59
60

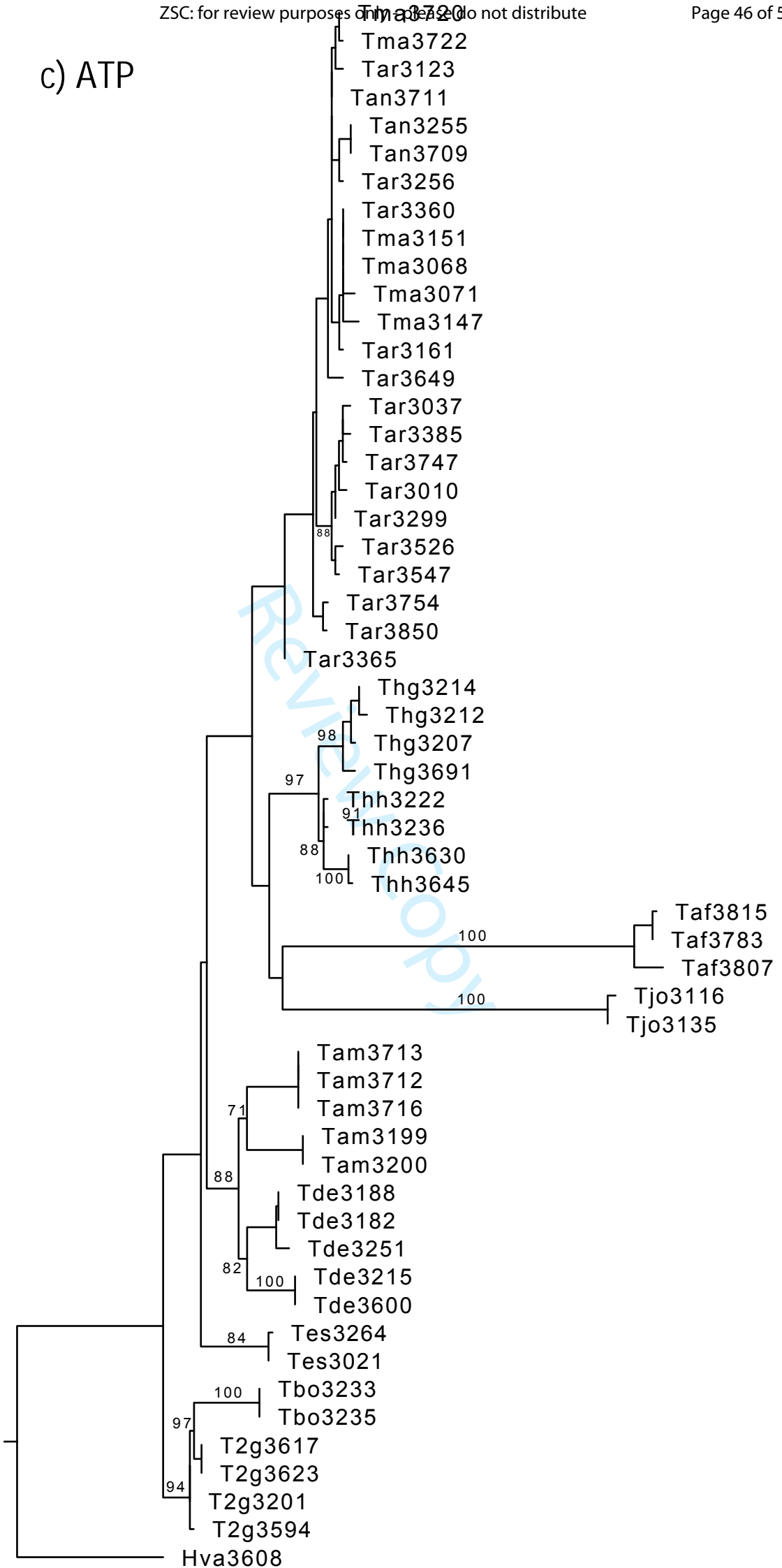
b) COI-CTL

1
2
3
4
5
6
7
8
9
10
11
12
13
14
15
16
17
18
19
20
21
22
23
24
25
26
27
28
29
30
31
32
33
34
35
36
37
38
39
40
41
42
43
44
45
46
47
48
49
50
51
52
53
54
55
56
57
58
59
60



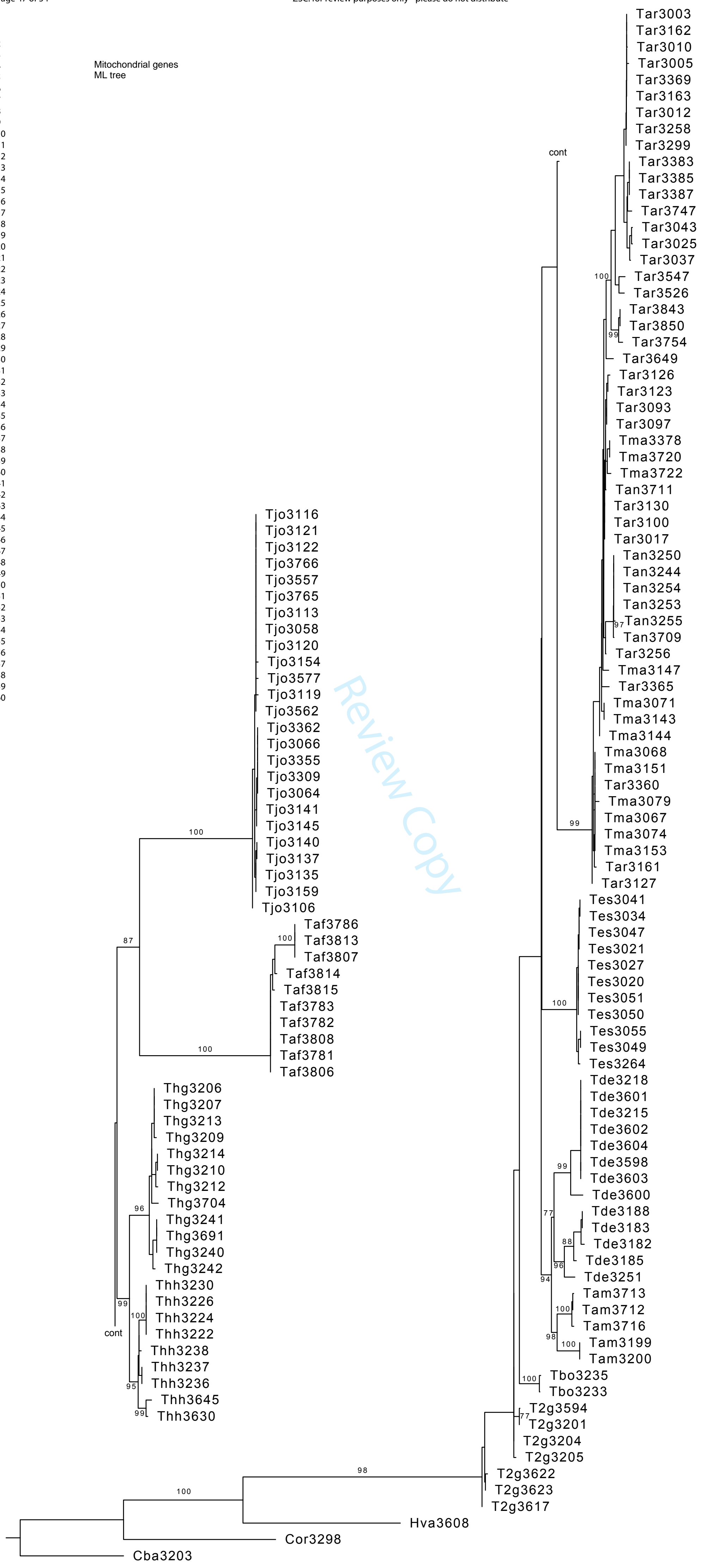
c) ATP

1
2
3
4
5
6
7
8
9
10
11
12
13
14
15
16
17
18
19
20
21
22
23
24
25
26
27
28
29
30
31
32
33
34
35
36
37
38
39
40
41
42
43
44
45
46
47
48
49
50
51
52
53
54
55
56
57
58
59
60



Mitochondrial genes
ML tree

1
2
3
4
5
6
7
8
9
10
11
12
13
14
15
16
17
18
19
20
21
22
23
24
25
26
27
28
29
30
31
32
33
34
35
36
37
38
39
40
41
42
43
44
45
46
47
48
49
50
51
52
53
54
55
56
57
58
59
60



Review Copy

D) Elongation Factor 1- α

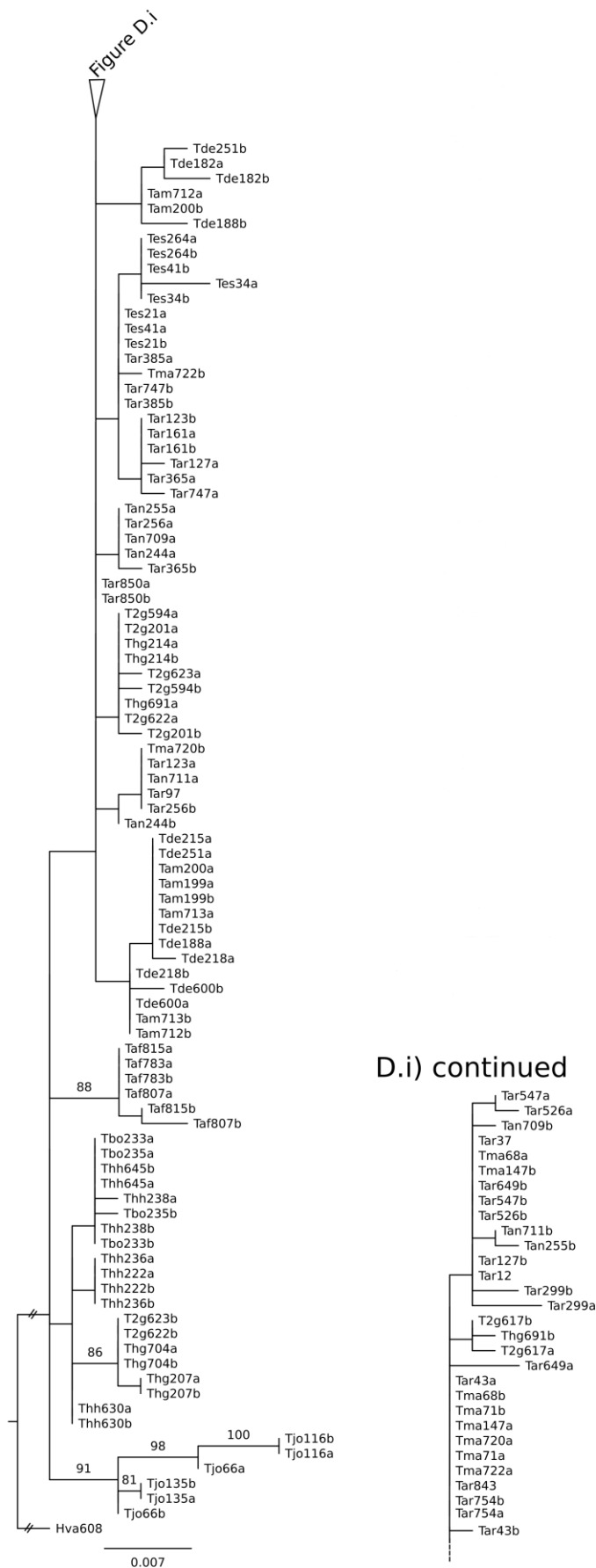


Figure S4. Maximum likelihood tree for the nuclear locus Elongation Factor 1- α .
ZSC submitted manuscript

Table S1. Specimens included in phylogenetic analyses, with codes, collection points, GPS coordinates and GenBank accession numbers. For nuclear EF1- α , when specimens were heterozygous, both haplotype accession numbers are listed, separated by a hyphen. Accession numbers starting with “M” or “ON” (marked in bold) were sequenced for this study. The remaining come from previous studies and are marked with ^a/^b/^c/, corresponding to Nunes *et al.* 2014a, Simões *et al.* 2014 and Costa *et al.* 2017, respectively.

Taxa	Code	Country	Locality	GPS coordinates	COI-Lep	COI-CTL	ATP	EF1- α
<i>T. afroamissa</i>	Taf781	Morocco	Chefchaouane	35.184, -5.224	KX582158 ^c			
<i>T. afroamissa</i>	Taf782	Morocco	Chefchaouane	35.184, -5.224	KX582159 ^c			
<i>T. afroamissa</i>	Taf783	Morocco	Chefchaouane	35.184, -5.224	KX582160 ^c		MG918037	MG978212
<i>T. afroamissa</i>	Taf786	Morocco	Afouzar	33.871, -4.029	KX582161 ^c			
<i>T. afroamissa</i>	Taf806	Morocco	Bni Hadifa	35.030, -4.164	KX582162 ^c			
<i>T. afroamissa</i>	Taf807	Morocco	Bni Hadifa	35.030, -4.164	KX582163 ^c		MG918038	MG978213-4
<i>T. afroamissa</i>	Taf808	Morocco	Bni Hadifa	35.030, -4.164	KX582164 ^c			
<i>T. afroamissa</i>	Taf813	Morocco	Targuist	34.965, -4.344	KX582165 ^c			
<i>T. afroamissa</i>	Taf814	Morocco	Tizi Tchen	34.929, -4.492	KX582166 ^c			
<i>T. afroamissa</i>	Taf815	Morocco	Tizi Tchen	34.929, -4.492	KX582167 ^c		MG918039	MG978215-6
<i>T. josei</i>	Tjo106	Portugal	Porches	37.136, -8.385	KC807272 ^a			
<i>T. josei</i>	Tjo113	Portugal	Porches	37.136, -8.385	KF977493 ^b			
<i>T. josei</i>	Tjo116	Portugal	Lagoa	37.136, -8.385	KC807271 ^a	MG918021	MG918080	MG978292
<i>T. josei</i>	Tjo119	Portugal	Budens	37.079, -8.837	KF977491 ^b			
<i>T. josei</i>	Tjo120	Portugal	Budens	37.073, -8.812	KC807267 ^a			
<i>T. josei</i>	Tjo121	Portugal	Budens	37.073, -8.812	KC807268 ^a	MG918022		
<i>T. josei</i>	Tjo122	Portugal	Budens	37.073, -8.812	KF977492 ^b			
<i>T. josei</i>	Tjo135	Portugal	Castro Marim	37.186, -7.484	KC807270 ^a	MG918023	MG918081	MG978293
<i>T. josei</i>	Tjo137	Portugal	Castro Marim	37.186, -7.484	KF977502 ^b	MG918024		
<i>T. josei</i>	Tjo140	Portugal	Castro Marim	37.186, -7.484	KC807269 ^a			
<i>T. josei</i>	Tjo141	Portugal	Moncarapacho	37.078, -7.821	KF977499 ^b	MG918025		
<i>T. josei</i>	Tjo145	Portugal	S. Brás de Alportel	37.137, -7.848	KF977498 ^b			
<i>T. josei</i>	Tjo154	Portugal	Moncarapacho	37.078, -7.821	KF977500 ^b			
<i>T. josei</i>	Tjo159	Portugal	Tavira	37.134, -7.635	KF977501 ^b			
<i>T. josei</i>	Tjo309	Portugal	Quinta do Lago	37.060, -8.021	KF977495 ^b			
<i>T. josei</i>	Tjo355	Portugal	Quinta do Lago	37.060, -8.021	KF977496 ^b			
<i>T. josei</i>	Tjo362	Portugal	Quinta do Lago	37.060, -8.021	KF977497 ^b			
<i>T. josei</i>	Tjo557	Spain	Cartaya	37.261, -7.129	KF977503 ^b			
<i>T. josei</i>	Tjo562	Spain	Cartaya	37.261, -7.129	KF977504 ^b			
<i>T. josei</i>	Tjo577	Spain	Cartaya	37.234, -7.066	KF977505 ^b			

1	<i>T. josei</i>	Tjo58	Portugal	Vale Judeu	37.128, -8.093	KC807273 ^a			
2	<i>T. josei</i>	Tjo64	Portugal	Vale Judeu	37.128, -8.093	KC807274 ^a	MG918020		
3	<i>T. josei</i>	Tjo66	Portugal	Vale Judeu	37.128, -8.093	KF977494 ^b			MG978294-5
4	<i>T. josei</i>	Tjo765	Portugal	Armação de Pêra	37.105, -8.361	MG905079			
5	<i>T. josei</i>	Tjo766	Portugal	Armação de Pêra	37.105, -8.361	MG905080			
6	<i>T. estrellae</i>	Tes21	Portugal	Braga	41.582, -8.321	KC807263 ^a	MG918006	MG918070	MG978275
7	<i>T. estrellae</i>	Tes20	Portugal	Braga	41.582, -8.321	MG905075			
8	<i>T. estrellae</i>	Tes27	Portugal	Braga	41.582, -8.321	KC807261 ^a			
9	<i>T. estrellae</i>	Tes34	Portugal	Braga	41.582, -8.321	MG905076	MG918007		MG978277-8
10	<i>T. estrellae</i>	Tes41	Portugal	Braga	41.582, -8.321	KC807264 ^a	MG918009		MG978279-80
11	<i>T. estrellae</i>	Tes47	Portugal	Amarante	41.243, -8.034	KC807262 ^a			
12	<i>T. estrellae</i>	Tes49	Portugal	Amarante	41.243, -8.034	MG905077			
13	<i>T. estrellae</i>	Tes50	Portugal	Amarante	41.244, -8.034	KC807260 ^a			
14	<i>T. estrellae</i>	Tes51	Portugal	Amarante	41.243, -8.034	KC807259 ^a			
15	<i>T. estrellae</i>	Tes55	Portugal	Amarante	41.243, -8.034	KC807266 ^a			
16	<i>T. estrellae</i>	Tes264	Portugal	Serra Estrela	40.355, -7.440	KC807265 ^a	MG918008	MG918071	MG978276
17	<i>T. h. galantei</i> type 1	Thg206	Spain	Capileira, Sierra Nevada	36.957, -3.353	KC807285 ^a			
18	<i>T. h. galantei</i> type 1	Thg207	Spain	Capileira, Sierra Nevada	36.957, -3.353	KC807282 ^a	MG918011	MG918072	MG978281
19	<i>T. h. galantei</i> type 1	Thg209	Spain	Capileira, Sierra Nevada	36.956, -3.347	KC807289 ^a			
20	<i>T. h. galantei</i> type 1	Thg210	Spain	Capileira, Sierra Nevada	36.956, -3.347	KC807291 ^a			
21	<i>T. h. galantei</i> type 1	Thg212	Spain	Capileira, Sierra Nevada	36.956, -3.347	KC807284 ^a		MG918073	
22	<i>T. h. galantei</i> type 1	Thg213	Spain	Capileira, Sierra Nevada	36.963, -3.341	KC807290 ^a			
23	<i>T. h. galantei</i> type 1	Thg214	Spain	Capileira, Sierra Nevada	36.963, -3.341	KC807286 ^a	MG918012	MG918074	MG978282
24	<i>T. h. galantei</i> type 1	Thg240	Spain	Laroles, Sierra Nevada	37.049, -3.017	KC807287 ^a			
25	<i>T. h. galantei</i> type 1	Thg241	Spain	Laroles, Sierra Nevada	37.049, -3.017	KC807283 ^a			
26	<i>T. h. galantei</i> type 1	Thg242	Spain	Laroles, Sierra Nevada	37.049, -3.017	KC807288 ^a			
27	<i>T. h. galantei</i> type 1	Thg691	Spain	Narila, Sierra Nevada	36.960, -3.175	ON470143	MG918015	MG918075	MG978283-4
28	<i>T. h. galantei</i> type 1	Thg704	Spain	Rubite	36.822, -3.335	MG905078			MG978285
29	<i>T. h. helianthemi</i>	Thh222	Spain	Cabo da Gata	36.838, -2.293	KC807292 ^a	MG918016	MG918076	MG978286
30	<i>T. h. helianthemi</i>	Thh224	Spain	Cabo da Gata	36.838, -2.293	KC807296 ^a			
31	<i>T. h. helianthemi</i>	Thh226	Spain	Cabo da Gata	36.838, -2.293	KC807294 ^a			
32	<i>T. h. helianthemi</i>	Thh230	Spain	Cabo da Gata	36.838, -2.293	KC807297 ^a			
33	<i>T. h. helianthemi</i>	Thh236	Spain	Vera	37.213, -1.900	KC807295 ^a	MG918017	MG918077	MG978287
34	<i>T. h. helianthemi</i>	Thh237	Spain	Vera	37.213, -1.900	KC807293 ^a			
35	<i>T. h. helianthemi</i>	Thh238	Spain	Vera	37.213, -1.900	KC807298 ^a			MG978288-9
36	<i>T. h. helianthemi</i>	Thh630	Spain	Sierra Filabres, north slope	37.366, -2.732	ON470142	MG918018	MG918078	MG978290

1	<i>T. h. helianthemi</i>	Thh645	Spain	Cantoria, Sierra Filabres	37.345, -2.199	ON470141	MG918019	MG918079	MG978291
2	<i>T. h. galantei</i> type 2	T2g201	Spain	Lanjarón, Sierra Nevada	36.923, -3.531	KC807279 ^a	MG918010	MG918033	MG978202-3
3	<i>T. h. galantei</i> type 2	T2g204	Spain	Lanjarón, Sierra Nevada	36.916, -3.504	KC807281 ^a			
4	<i>T. h. galantei</i> type 2	T2g205	Spain	Lanjarón, Sierra Nevada	36.916, -3.504	KC807280 ^a			
5	<i>T. h. galantei</i> type 2	T2g594	Spain	W Lanjarón, Sierra Nevada,	36.923, -3.531	MH248134	MG918013	MG918034	MG978204-5
6	<i>T. h. galantei</i> type 2	T2g617	Spain	Pinos Genil, Sierra Nevada	37.138, -3.476	MH248135		MG918035	MG978206-7
7	<i>T. h. galantei</i> type 2	T2g622	Spain	Pinos Genil, Sierra Nevada	37.138, -3.476	MG905049			MG978208-9
8	<i>T. h. galantei</i> type 2	T2g623	Spain	Pinos Genil, Sierra Nevada	37.138, -3.476	ON470144	MG918014	MG918036	MG978210-11
9	<i>T. bouhardi</i>	Tbo233	Spain	Campico de los López, Murcia	37.583, -1.571	KC807276 ^a	MG917999	MG918063	MG978261
10	<i>T. bouhardi</i>	Tbo235	Spain	Campico de los López, Murcia	37.583, -1.571	KC807275 ^a	MG918000	MG918064	MG978262-3
11	<i>T. armandi</i>	Tam199	Spain	Gibraltar	36.188, -5.359	KC807277 ^a	MG917973	MG918040	MG978217
12	<i>T. armandi</i>	Tam200	Spain	Gibraltar	36.188, -5.359	KC807278 ^a	MG917974	MG918041	MG978218-9
13	<i>T. armandi</i>	Tam712	Spain	Estella del Marques	36.685, -6.063	MG905050	MG917975	MG918042	MG978220-1
14	<i>T. armandi</i>	Tam713	Spain	Estella del Marques	36.685, -6.063	MG905051	MG917976	MG918043	MG978222-3
15	<i>T. armandi</i>	Tam716	Spain	Estella del Marques	36.685, -6.063	MG905052	MG917977	MG918044	
16	<i>T. defauti</i>	Tde182	Spain	Puerto del Viento, Ronda	36.787, -5.053	KC807305 ^a	MG918001	MG918065	MG978264-5
17	<i>T. defauti</i>	Tde183	Spain	Puerto del Viento, Ronda	36.787, -5.053	KC807307 ^a			
18	<i>T. defauti</i>	Tde185	Spain	Puerto del Viento, Ronda	36.787, -5.053	KC807309 ^a			
19	<i>T. defauti</i>	Tde188	Spain	Puerto del Viento, Ronda	36.787, -5.053	KC807308 ^a	MG918002	MG918066	MG978266-7
20	<i>T. defauti</i>	Tde215	Spain	Sierra Nevada	37.138, -3.468	KC807310 ^a	MG918003	MG918067	MG978268
21	<i>T. defauti</i>	Tde218	Spain	Sierra Nevada	37.138, -3.468	KC807304 ^a			MG978269-70
22	<i>T. defauti</i>	Tde251	Spain	Zagra	37.283, -4.234	KC807306 ^a	MG918004	MG918068	MG978271-2
23	<i>T. defauti</i>	Tde598	Spain	Sierra Nevada	37.138, -3.476	MG905069			
24	<i>T. defauti</i>	Tde600	Spain	Sierra Nevada	37.138, -3.476	MG905070	MG918005	MG918069	MG978273-4
25	<i>T. defauti</i>	Tde601	Spain	Sierra Nevada	37.138, -3.476	MG905071			
26	<i>T. defauti</i>	Tde602	Spain	Sierra Nevada	37.138, -3.476	MG905072			
27	<i>T. defauti</i>	Tde603	Spain	Sierra Nevada	37.138, -3.476	MG905073			
28	<i>T. defauti</i>	Tde604	Spain	Sierra Nevada	37.138, -3.476	MG905074			
29	<i>T. aneabi</i>	Tan244	Spain	Granada	37.256, -3.482	KC807300 ^a			MG978224-5
30	<i>T. aneabi</i>	Tan250	Spain	Zagra	37.283, -4.234	KC807301 ^a			
31	<i>T. aneabi</i>	Tan253	Spain	Zagra	37.283, -4.234	KC807303 ^a			
32	<i>T. aneabi</i>	Tan254	Spain	Zagra	37.283, -4.234	KC807302 ^a			
33	<i>T. aneabi</i>	Tan255	Spain	Zagra	37.283, -4.234	KC807299 ^a	MG917978	MG918045	MG978226-7
34	<i>T. aneabi</i>	Tan709	Spain	Frailles	37.508, -3.832	MG905053	MG917979	MG918046	MG978228-9
35	<i>T. aneabi</i>	Tan711	Spain	Estepa	37.366, -4.818	MG905054	MG917980	MG918047	MG978230-1
36	<i>T. mariae</i>	Tma143	Portugal	Vale do Lobo	37.061, -8.061	KC807253 ^a			

1	<i>T. mariae</i>	Tma144	Portugal	Vale do Lobo	37.061, -8.061	KC807249 ^a	MG918028		
2	<i>T. mariae</i>	Tma147	Portugal	Vale do Lobo	37.061, -8.061	KC807255 ^a	MG918029	MG918082	MG978296-7
3	<i>T. mariae</i>	Tma151	Portugal	Vale do Lobo	37.061, -8.061	KC807250 ^a		MG918083	
4	<i>T. mariae</i>	Tma153	Portugal	Vale do Lobo	37.061, -8.061	KC807257 ^a			
5	<i>T. mariae</i>	Tma378	Spain	Cartaya	37.262, -7.130	MG905083			
6	<i>T. mariae</i>	Tma67	Portugal	Vale Judeu	37.106, -8.095	KC807258 ^a			
7	<i>T. mariae</i>	Tma68	Portugal	Vale Judeu	37.106, -8.095	KC807251 ^a	MG918026	MG918084	MG978298-9
8	<i>T. mariae</i>	Tma71	Portugal	Vale Judeu	37.106, -8.095	KC807254 ^a	MG918027	MG918085	MG978300
9	<i>T. mariae</i>	Tma720	Spain	Huelva	37.226, -7.035	MG905082	MG918030	MG918086	MG978301-2
10	<i>T. mariae</i>	Tma722	Spain	Huelva	37.226, -7.035	MG905083	MG918031	MG918087	MG978303-4
11	<i>T. mariae</i>	Tma74	Portugal	Vale Judeu	37.106, -8.095	KC807252 ^a			
12	<i>T. mariae</i>	Tma79	Portugal	Vale Judeu	37.106, -8.095	KC807256 ^a			
13	<i>T. mariae</i>	Tma79	Portugal	Vale Judeu	37.106, -8.095	KC807256 ^a			
14	<i>T. argentata</i> North clade	Tar3	Portugal	Sesimbra	38.447, -9.086	KC807243 ^a			
15	<i>T. argentata</i> North clade	Tar5	Portugal	Sesimbra	38.443, -9.089	KC807245 ^a			
16	<i>T. argentata</i> North clade	Tar10	Portugal	Sesimbra	38.443, -9.089	KC807244 ^a	MG917981	MG918048	
17	<i>T. argentata</i> North clade	Tar12	Portugal	Sesimbra	38.445, -9.091	MG905055	MG917982		MG978232
18	<i>T. argentata</i> North clade	Tar25	Portugal	Braga	41.582, -8.321	KC807230 ^a	MG917983		
19	<i>T. argentata</i> North clade	Tar37	Portugal	Braga	41.582, -8.321	MG905061	MG917984	MG918055	MG978245
20	<i>T. argentata</i> North clade	Tar43	Portugal	Braga	41.582, -8.321	KC807229 ^a	MG917985		MG978247-8
21	<i>T. argentata</i> North clade	Tar43	Portugal	Braga	41.582, -8.321	KC807229 ^a	MG917985		MG978247-8
22	<i>T. argentata</i> North clade	Tar162	France	Bouzigues	43.455, 3.657	KC807233 ^a			
23	<i>T. argentata</i> North clade	Tar163	France	Narbonne	43.155, 2.964	KC807234 ^a			
24	<i>T. argentata</i> North clade	Tar299	Portugal	Serra d'Aire & Candeeiros	39.456, -8.800	MG905058	MG917990	MG918052	MG978241-42
25	<i>T. argentata</i> North clade	Tar383	Italy	Benne, Piedmont	45.281, 7.541	KC807237 ^a			
26	<i>T. argentata</i> North clade	Tar385	Italy	Serradica, Marche	43.278, 12.847	KC807236 ^a	MG917992	MG918056	MG978246
27	<i>T. argentata</i> North clade	Tar387	Italy	Cella, Lombardy	44.780, 9.187	KC807235 ^a			
28	<i>T. argentata</i> North clade	Tar747	Italy	Pietrafitta, Calabria	39.249, 16.340	MG905064	MG917996	MG918060	MG978255-6
29	<i>T. argentata</i> North clade	Tar747	Italy	Pietrafitta, Calabria	39.249, 16.340	MG905064	MG917996	MG918060	MG978255-6
30	<i>T. argentata</i> South clade	Tar17	Portugal	Portel	38.303, -7.709	KC807238 ^a			
31	<i>T. argentata</i> South clade	Tar93	Portugal	Portel	38.303, -7.709	KC807239 ^a			
32	<i>T. argentata</i> South clade	Tar97	Portugal	Portel	38.303, -7.709	MG905068			MG978260
33	<i>T. argentata</i> South clade	Tar97	Portugal	Portel	38.303, -7.709	MG905068			MG978260
34	<i>T. argentata</i> South clade	Tar100	Portugal	Portel	38.303, -7.709	KC807248 ^a			
35	<i>T. argentata</i> South clade	Tar123	Portugal	S. Bartolomeu de Messines	37.257, -8.297	KC807240 ^a	MG917986	MG918049	MG978233-4
36	<i>T. argentata</i> South clade	Tar126	Portugal	S. Bartolomeu de Messines	37.257, -8.297	KC807242 ^a			
37	<i>T. argentata</i> South clade	Tar127	Portugal	S. Bartolomeu de Messines	37.257, -8.297	MG905056			MG978235-6
38	<i>T. argentata</i> South clade	Tar127	Portugal	S. Bartolomeu de Messines	37.257, -8.297	MG905056			MG978235-6
39	<i>T. argentata</i> South clade	Tar130	Portugal	S. Bartolomeu de Messines	37.257, -8.297	KC807241 ^a	MG917987		
40	<i>T. argentata</i> South clade	Tar130	Portugal	S. Bartolomeu de Messines	37.257, -8.297	KC807241 ^a	MG917987		
41	<i>T. argentata</i> South clade	Tar161	Portugal	Moncarapacho	37.078, -7.821	MG905057	MG917988	MG918050	MG978238
42	<i>T. argentata</i> South clade	Tar256	Spain	Espiel	38.194, -5.027	KC807232 ^a	MG917989	MG918051	MG978239-40

1	<i>T. argentata</i> South clade	Tar258	Spain	Espiel	38.194, -5.027	KC807231 ^a			
2	<i>T. argentata</i> South clade	Tar360	Portugal	Mata Lobo	37.080, -7.949	MG905059		MG918053	
3	<i>T. argentata</i> South clade	Tar365	Spain	Ayamonte	37.276, -7.342	KC807246 ^a	MG917991	MG918054	MG978243-44
4	<i>T. argentata</i> South clade	Tar369	Spain	Ayamonte	37.276, -7.342	KC807247 ^a			
5	<i>T. argentata</i> South clade	Tar649	Spain	Oria	37.497, -2.292	MG905060	MG917995	MG918059	MG978253-4
6	<i>T. argentata</i> Central clade	Tar526	Spain	Almaraz	39.760, -5.735	MG905062	MG917993	MG918057	MG978249-50
7	<i>T. argentata</i> Central clade	Tar547	Spain	Albarracín	40.425, -1.381	MG905063	MG917994	MG918058	MG978251-2
8	<i>T. argentata</i> Catalonia clade	Tar843	Spain	Girona	42.057, 2.991	MG905066	MG917997		MG978258
9	<i>T. argentata</i> Catalonia clade	Tar850	Spain	Catalonia	42.069, 3.107	MG905067	MG917998	MG918062	MG978259
10	<i>T. argentata</i> Catalonia clade	Tar754	Spain	Alicante	38.634, -0.523	MG905065		MG918061	MG978257
11	<i>Cicada barbara</i>	Cba203	Spain	Lanjarón, Sierra Nevada	36.916, -3.504	KC807317 ^a	MG917971		
12	<i>Cicada orni</i>	Cor298	Spain	Serra d'Aire & Candeeiros	39.455, -8.752	KC807318 ^a			
13	<i>Hilaphura varipes</i>	Hva608	Spain	Pinos Genil, Sierra Nevada	37.138, -3.476	KX582168 ^c	MG917972	MG918032	MG978201
14	<i>Maoricicada cassiope</i>	Mcass14	New Zealand	-	-				
15									
16									
17									
18									
19									
20									
21									
22									
23									
24									
25									
26									
27									
28									
29									
30									
31									
32									
33									
34									
35									
36									
37									
38									
39									
40									
41									
42									
43									
44									
45									
46									

- view Copy

Table S2. Primers and annealing temperature used to amplify each locus.

Gene	Primers	Primer sequence (from 5' to 3')	References	Product length (bp)	T _{annealing} (°C)
Mitochondrial loci					
Cytochrome oxidase I (COI-Lep) 5' region	LepF	ATT CAA CCA ATC ATA AAG ATA TTG G	Hajibabaei <i>et al.</i> (2006)	650	45
	LepR	TAA ACT TCT GGA TGT CCA AAA AAT CA	Hajibabaei <i>et al.</i> (2006)		
Cytochrome oxidase I (COI-CTL) 3' region	C1-J-2195	TTG ATT TTT TGG TCA TCC AGA AGT	Simon <i>et al.</i> (1994)	850	53
	TL2-N-3014	TCC AAT GCA CTA ATC TGC CAT ATT A	Simon <i>et al.</i> (1994)		
ATP synthetase A6/A8	TK-J-3799_for A6A8_rev	GGC TGA AAG TAA GTA ATG GTC TCT ATG RCC AGC AAT TAT ATT AGC TG	Buckley <i>et al.</i> (2001) modified from Marshall <i>et al.</i> (2008)	800	57
Nuclear loci					
Elongation factor 1 α	EF1a-97_for	ACG CCC CTG GAC ATA GAG AT	Buckley <i>et al.</i> (2006)	600	60
	EF1a-189_rev	CAA CCT GAG ATT GGC ACA AA	Buckley <i>et al.</i> (2006)		